Internalization and desensitization of the human glucose-dependent-insulinotropic receptor is affected by N-terminal acetylation of the agonist

Accepted Manuscript

Internalization and desensitization of the human glucose-dependent-insulinotropic receptor is affected by N-terminal acetylation of the agonist

Sadek Ismail, Ingrid Dubois-Vedrenne, Marie Laval, Irina Tikhonova, Romina D'Angelo, Claire Sanchez, Pascal Clerc, Marie-Julie Gherardi, Véronique Gigoux, Remi Magnan, Daniel Fourmy

PII: S0303-7207(15)30010-1

DOI: 10.1016/j.mce.2015.07.001

Reference: MCE 9209

To appear in: *Molecular and Cellular Endocrinology*

Received Date: 15 May 2015

Revised Date: 30 June 2015

Accepted Date: 1 July 2015

Please cite this article as: Ismail, S., Dubois-Vedrenne, I., Laval, M., Tikhonova, I., D'Angelo, R., Sanchez, C., Clerc, P., Gherardi, M.-J., Gigoux, V., Magnan, R., Fourmy, D., Internalization and desensitization of the human glucose-dependent-insulinotropic receptor is affected by N-terminal acetylation of the agonist, *Molecular and Cellular Endocrinology* (2015), doi: 10.1016/j.mce.2015.07.001.

Internalization and desensitization of the human glucose-dependent-insulinotropic receptor is affected by N-terminal acetylation of the agonist

Sadek Ismail[1], Ingrid Dubois-Vedrenne[1], Marie Laval[1], Irina Tikhonova[2], Romina D'Angelo[3], Claire Sanchez[1], Pascal Clerc[1], Marie-Julie Gherardi[1], Véronique Gigoux[1], Remi Magnan[1] and Daniel Fourmy[1]

1. Université de Toulouse 3, EA 4552, INSERM U1048/I2MC, Toulouse, France.
2. Molecular Therapeutics, School of Pharmacy, Queen's University of Belfast, North Ireland, UK
3. Cellular Imaging Facility Rangueil, INSERM U1048/I2MC, Toulouse, France.

Corresponding author: Daniel Fourmy, EA 4552 Inserm U1048/I2MC, 1 avenue Jean Poulhès, BP 84225, 31432 Toulouse Cedex 4. Phone: 33 5 61 32 30 57; Email: Daniel.Fourmy@inserm.fr

Abstract

How incretins regulate presence of their receptors at the cell surface and their activity is of paramount importance for the development of therapeutic strategies targeting these receptors. We have studied internalization of the human Glucose-Insulinotropic Polypeptide receptor (GIPR). GIP stimulated rapid robust internalization of the GIPR, the major part being directed to lysosomes. GIPR internalization involved mainly clathrin-coated pits, AP-2 and dynamin. However, neither GIPR C-terminal region nor β-arrestin1/2 was required. Finally, N-acetyl-GIP recognized as a dipeptidyl-IV resistant analogue, fully stimulated cAMP production with a ~15-fold lower potency than GIP and weakly stimulated GIPR internalization and desensitization of cAMP response. Furthermore, docking N-acetyl-GIP in the binding site of modelled GIPR showed slighter interactions with residues of helices 6 and 7 of GIPR compared to GIP. Therefore, incomplete or partial activity of N-acetyl-GIP on signaling involved in GIPR desensitization and internalization contributes to the enhanced incretin activity of this peptide.

Keywords: glucose-dependent insulinotropic polypeptide, internalization, desensitization, cAMP signaling, BRET, fluorescence confocal microscopy, molecular modeling, biased agonist

Abbreviations: GIP, glucose-dependent insulinotropic polypeptide; GIPR, glucose-dependent insulinotropic polypeptide receptor; BRET, Bioluminescence Resonance Energy Transfer

1. Introduction

Glucose-dependent insulinotropic polypeptide (GIP) is released by the entero-endocrine K cells from the proximal duodenum [1,2]. GIP stimulates insulin secretion from pancreatic β-cells after ingestion of nutrients. GIP, together with Glucagon-like peptide 1 (GLP1), contributes for 50 to 70 percent to post-prandial insulin secretion [3]. GIP further enhances its glucose-lowering effects by the inhibition of hepatic glucose production and the stimulation of proinsulin gene transcription and translation. Moreover, GIP is known to play a role in lipid metabolism and fat deposition. Indeed, GIP increases lipoprotein lipase activity, stimulates lipogenesis, enhances fatty acid and glucose uptake in adipocytes [3]. GIP exerts its physiological functions through binding to GIP receptor (GIPR) which belongs to subfamily-2 of G-protein-coupled receptors (GPCR) [4,5]. GIPR triggers Gs-mediated cAMP production and subsequent signaling cascades [3].

Until very recently, one major argument against the development of a therapeutic strategy using GIP analogues to treat diabetes 2 was raised by the impairment of GIP-dependent insulin secretion in diabetic type II patients, with an almost complete loss of amplification of the second phase of insulin secretion [6-10]. This detrimental effect was found to result from down-regulation of GIPR presence in pancreatic β-cells exposed to diabetic milieu. Conversely, recent reports indicated that glycemia normalization in diabetic animals and humans significantly improves GIP-stimulated insulin secretion [11,12]. Moreover, very promising pre-clinical data were obtained in rodents, monkeys and humans showing that a single peptidic molecule having dual agonist activity at GIP and GLP1 receptors exhibits enhanced insulinotropic and anti-hyperglycemic efficacy relative to GLP1 alone [13]. As a consequence, a renewed interest in developing pharmacological strategies to target GIPR has emerged [13-15].

So far, regulation of GIPR presence at the cell surface remains poorly understood. First, although exposure of pancreatic islet cells to GIP has been shown to produce homologous desensitization of the GIP receptor, the impact of GIPR internalization and trafficking on GIPR-dependent response and the underlying molecular mechanisms have not been investigated in detail yet [16,17]. Recently, it has been reported that in 3T3-L1 adipocytes, GIPR constitutively internalizes and recycles to the cell surface and that GIP induces a down-regulation of plasma membrane GIPR by slowing GIPR recycling without affecting kinetics of GIPR internalization [18]. Accordingly, GIPR does not conform to the typical behavior of G-protein coupled receptors which has been essentially studied for members of rhodopsin-related GPCRs (sub-family 1) and much less frequently for members of sub-family 2 of GPCRs such as the GIPR [19,20].

In most cases, agonist-induced internalization of GPCRs starts with the action of GPCRs kinases (GRKs) that selectively phosphorylate agonist-activated receptors. Phosphorylation of the receptors and subsequent binding of arrestins terminate the G-protein-mediated signal of the membrane receptors. Arrestin-bound membrane receptors are then rapidly targeted to the clathrin-coated pits, thereby promoting their internalization [20,21]. Furthermore, it has been recognized that in addition to

its role in desensitization of G-protein mediated signal and cell responsiveness, β-arrestins trigger signaling pathways independently of G-protein coupling [22]. Importantly, pharmacological agents, named “biased ligands”, have been discovered, which activate differentially G-protein-dependent and arrestin-dependent signaling pathways [23].

In this context, the aim of this study was to investigate internalization of GIPR following agonist exposure, as well as cellular and molecular underlying mechanisms. Besides, this study enabled the identification of a GIP analogue, N-acetyl-GIP, so far recognized as a dipeptidyl-IV resistant GIP analogue, which fully stimulated cAMP production but with a ~15-fold lower potency than GIP. Furthermore, N-acetyl-GIP only weakly induced internalization of the GIPR and desensitization of GIPR-dependent cAMP response.

2. Materials and methods

2.1. Materials

Fragment 1-30 of human GIP (termed GIP) was synthesized as previously described [24]. N-acetyl-GIP(1-30) (termed N-acetyl-GIP) was from Millegen (Toulouse, France). Alexa Fluor 647 labeled-GIP (termed AlexaF647-GIP) and Alexa Fluor 647 labeled–acetyl-GIP(1-30) (termed AlexaF647-N-acetyl-GIP) were obtained according to the procedure described [24]. In both peptides, Alexa Fluor 647 moiety was coupled to the peptide and coupling products were HPLC purified. Peak corresponding to peptide in which Alexa Fluor 647 was attached to Lysine 30, as determined by Maldi Tof analysis, was selected [24]. Both fluorescent probes were highly specific of GIPR (less than 5% nonspecific labeling in the present of 100-fold excess of unlabeled peptide). Radio-labeled GIP was obtained by radio-iodination of Phe^1-GIP(1-30) with ^{125}I-Na (Perkin Elmer, France) in the presence of chloramine T and was HPLC purified on a C-18 column. ^{125}I-Phe^1-GIP bound to a single class of GIPR binding sites from HEK 293T or Flp-In^{TM}GIPR-293 cells with a dissociation constant, Kd of 75.7 ± 8.4 nM. Sequence encoding short variant of the human GIPR was derived from a plasmid kindly given by Professor Bernard Thorens (Lausanne, Switzerland). Chemicals were from the following sources: dynasore from Calbiochem, Pitstop2 from Abcam, Filipin and H89 from Sigma-Aldrich, LysoTracker® Red from Invitrogen.

The cDNAs encoding GIPR, green fluorescent protein (GFP) tagged GIPRs and Renilla luciferase (Rluc) fused GIPR were generated by subcloning respectively the GIPR cDNA in pcDNA5/FTR (Invitrogen), pEGFP-N1 (BD biosciences clontech), pRluc-N1(h) (Perkin Elmer). DsRed tagged Rab5, DsRed tagged Rab11, DsRed tagged Rab7, Clathrin-LCa-eYFP and Caveoline1-GFP were obtained from Addgene (www.addgene.org). Plasmids encoding green fluorescent protein (GFP) tagged β-arrestin1 (β-arrestin1 = arrestin2), yellow fluorescent protein (YFP) tagged β-arrestin1, yellow fluorescent protein (YFP) tagged β-arrestin2 (β-arrestin2 = arrestin3), Rluc-EPAC-YFP and D44A-dynamin were generous gifts from Marc Caron (Duke University Medical Center, Durham, USA). Green fluorescent protein (GFP) tagged β-arrestin2, kindly given by Robert Lefkowitz (Duke

University Medical Center, Durham, USA), was subcloned in pcDNA5/FRT. Plasmid encoding YFP tagged β-adaptin2 was given by Professor Michel Bouvier (Montreal University, Canada). All truncated receptor cDNAs at C-terminal tail (TR414, TR432 and TR452) and the GFP tagged GIPR constructs were obtained by insertion of a stop codon or linker sequence, respectively. All constructs were sequenced before use.

2.2. Cell lines and transfections

HEK 293 cells stably expressing the GIPR (Flp-ln™ HEK-GIPR) and the CCK2R (Flp-ln™ HEK-CCK2R) were obtained using the Flp-In™ system (Invitrogen). Alternatively, HEK293T transiently expressing the GIPR were used. All HEK293 derived cell lines cells were maintained in Dulbecco's Modified Eagle's medium supplemented with 10% of fetal bovine serum (FBS), in a humidified atmosphere at 95% air and 5% CO2. MIN-6-B1clone (kindly given by Doctor Jun-Ichi Miyazaki) was maintained in culture in Dulbecco's Modified Eagle's medium 25mM glucose supplemented with 15% of FBS, 71 µM 2-mercaptoethenol. Transfections were performed using polyethylenimine (PEI) transfection reagent (1mg/mL, pH 7.4) (Polyplus). Plasmids were diluted in DMEM without FBS (ratio DNA (µg) / PEI (µL) 1:3). The mixture was mixed for 15 sec on a vortex, incubated for 15 min at room temperature and then deposited on the cells.

2.3. Confocal fluorescence microscopy

Cells were plated onto poly-L-lysine (Sigma-Aldrich) coated 4-wells Lab-Tek chambered coverglass (Nunc). After an overnight growth, cells were transfected either with 1 µg/well of pcDNA5/FRT containing cDNAs of interest. 24 hours later, the culture medium was replaced by D-PBS (Dulbecco's PBS1X, 1mg/L glucose, 36mg/L sodium pyruvate, pH 7.4, calcium and magnesium free). Cells were stimulated with appropriate ligands and confocal microscopy images of GFP, DsRed or Alexa Fluor 647 fluorescence, were collected by using single- or double-line excitation (respectively 488 nm, 543nm, 633nm) on a Zeiss Laser Scanning Microscope LSM-510 or Zeiss Laser Scanning Microscope LSM-780 at 37°C. Concentrations of fluorescent GIP analogues equal or above 10 nM were used in internalization and trafficking studies because confocal microscopy and FACS did not enable detection of cell-associated fluorescence at lower concentrations. For β-arrestin1-GFP and β-arrestin2-GFP membrane recruitment assays, time series over a 5 min period were performed (pictures were taken every 30 seconds) and the decrease of cytoplasmic fluorescence was measured using the Region of interest (ROI) function of LSM-510 software.

2.4. Quantification of internalization and recycling by flow cytometry

Flp-In™GIPR-293 cells or HEK293T cells were plated onto poly-L-lysine coated 24-wells plates. After an overnight growth, cells were incubated with AlexaF647-GIP (100 nM) in PBS 0.2% for various times (from 5 to 60 min). Cells were washed twice with cold PBS 0.2% BSA and acid washed (0.2M acetic acid, 0.5 M NaCl, pH 2.5) for 10 min on ice. Cells were then washed twice with PBS 0.2% BSA and detached for transfer to FACS tubes. Cell-associated fluorescence was determined

using a BD FACSCalibur™ flow cytometer, with Flp-In™ 293 that do not express GIPR as a negative control.

For recycling assay, cells were incubated with 100 nM GIP in DMEM/HEPES (20mM) for 1 hour at 37°C to enable GIPR internalization. Cells were washed 3 times with DMEM/HEPES and incubated without ligand for increasing times in order to enable GIPR recycling. GIPR at the cell surface were identified with AlexaF647-GIP (1µM) for 45 min at 37°C in the presence of the internalization inhibitor, dynasore (100 µM) added 5 min before the ligand.

2.5. BRET assays of β-arrestin recruitment and cAMP production

HEK 293T or Flp-In™GIPR-293 cells were plated onto 10-cm culture dishes and overnight grown. For β-arrestin recruitment assays, cells were transfected with 0.2µg of Rluc tagged GIPR and 10µg of either β-arrestin1-YFP or β-arrestin2- YFP. For cAMP measurements, Flp-In™GIPR-293 cells were transfected with 5µg of Epac biosensor. Alternatively, HEK 293T cells were co-transfected with 5 µg of Epac biosensor and 1 µg of GIP receptors. 24 hours after transfection, cells were plated in 96-wells clear bottom plates (Corning) at a density of 100.000 cells per well in phenol red free DMEM 2% FBS. After an overnight incubation, the medium was removed and replaced by calcium and magnesium free PBS. BRET assay was initiated by adding 10 µl of coelenterazine h to the wells (final concentration 5 µM). After 5 min of incubation with coelenterazine h, GIP, N-acetyl-GIP or Forskolin was added. Readings started 5 min after the addition of GIP or N-acetyl-GIP. A Mithras LB940 instrument (Berthold) that allows the sequential integration of signals at 465 to 505 nm and 515 to 555 nm windows and MicroWin 2000 software were used.

2.6. Receptor binding assays

Flp-In™GIPR-293 cells grown overnight were onto 10-cm culture dishes. 24 h later, cells were transferred to 24-well plates. Approximately 24 h later, binding assays were performed using ^{125}I-Phe^{1}-GIP according to the protocol previously described in detail [25]. Ki for competitors were calculated according to the equation Ki = IC_{50}/1+[^{125}I-Phe^{1}-GIP]/Kd (^{125}I-Phe^{1}-GIP) in which IC_{50} (concentration inhibiting half of specific binding) and Kd of ^{125}I-Phe^{1}-GIP were calculated using the non-linear curve fitting software GraphPad Prism (San Diego, CA).

2.7. cAMP-desensitization assay

Flp-In™GIPR-293 cells transfected with Epac biosensor and plated in 96-well clear bottom plates were pre-stimulated at 37°C for increasing times by GIP (0.1 µM) or N-acetyl-GIP (1 µM) with or without H89 (10 µM). Then, pre-stimulation was stopped by removing the medium. GIP peptides were washed out from cells (two times) with PBS buffer containing 0.5% BSA. cAMP production in response to a second challenge with 1µM GIP or 10 µM N-acetyl-GIP was measured by BRET as indicated above. cAMP levels were expressed as the percent of cAMP in cells which were not pre-stimulated with peptides.

2.8. Insulin secretion from MIN-6-B1cells

Insulinoma cells were seeded on 24-wells plates (3.10^5 cells/well) and let to grow for 48h. Cells were then washed 3-times with 500 µL KRBH buffer pH: 7.4 (125 mM NaCl, 4.74 KCl, 1 mM $CaCl_2$, 1.2 mM KH_2PO_4, 1.2 mM $MgSO_4$, 5mM $NaHCO_3$, 10 mM, Hepes, 0.1% BSA). Cells were incubated for 2h at 37°C in KRH buffer supplemented with 2.8 mM glucose. The incubation medium was discarded and replaced with 500 µL buffer containing 11 mM glucose with or without GIP or N-acetyl-GIP. Cells were let to secrete insulin during 2h. Supernatants were centrifuged for 5 min at 2000 rpm to eliminate detached cells, and secreted insulin contained in supernatants was determined using Ultrasensitive Insulin Elisa Kit (Alpco) according to manufacturer instructions. Insulin secretion was expressed as -fold basal value obtained in the absence of GIP analogue.

2.9. Molecular modeling

The crystal structure of the human glucagon receptor (GCGR) with PDB code of 4L6R was used to build the homology model of the GIPR helical bundle using Prime 3.8 with the energy-based method [26]. The N-terminal domain of GIPR bound to GIP with PDB code of 2QKH was docked to the helical bundle taking into account the previously identified interactions between the N terminal domain of GIP and the residues of the GIPR helical bundle [24,27]. The docking was done in two steps. Firstly, the first five amino acid residues of the N terminal domain was docked with the Induced Fit protocol, where docking was constrained around residues known to be important for binding from mutagenesis. Next, the remaining part of GIP together with the N terminal domain of GIPR was assembled manually and subjected to 500 ps minimization followed by 1000 ps of molecular simulations in implicit environment. MacroModel 9.9 was used for all minimizations and simulations. Images with the molecular models were prepared with Maestro 9.9.

2.10. Statistics

All values are expressed as the mean +/- standard error of the mean (SEM). Statistical analyses of data using One- or two-way ANOVA with Dunnett's or Turkeys's comparison test were performed using GraphPad Prism version 6.0. In figures and table 1, significance degrees were given as following: * $0.01<p<0.05$; ** $0.001<p<0.01$; ***$p<0.001$ or • $0.01<p<0.05$; •• $0.001<p<0.01$; •••$p<0.001$.

3. Results

3.1. GIP receptors rapidly and abundantly internalize following GIP stimulation

Flp-ln™ HEK-GIPR and HEK293T-GIPR cells used for studies of internalization and trafficking of GIPR were characterized prior to their use as biological tools. As shown on Supplemental figure 1S, cAMP levels measured by BRET using EPAC sensor were dose-dependently increased upon stimulation by GIP, with half-maximal stimulation (EC_{50}) in the nanomolar range. Therefore, GIPR appeared correctly coupled to adenylyl cyclase in the two cell lines. Moreover, cAMP production measured with EPAC sensor was in agreement with that measured using a radio-immunoassay [24] thus validating BRET assay to measure cAMP. We also characterized pharmacologically AlexaF647-GIP which was used to study internalization and intracellular trafficking of GIPR. As shown on supplemental Fig 1S and table 1, alexaF647-GIP bound to Flp-ln™ HEK-GIPR cells and stimulated production of cAMP similarly to GIP. Moreover, fluorescence labeling of GIPR by alexaF647-GIP was highly specific since FACS analysis of Flp-ln™ HEK-GIPR cells incubated with alexaF647-GIP in the presence 1 µM unlabeled GIP revealed less than 5% of nonsaturable labeling (not illustrated).
Confocal microscopy observations of Flp-ln™ HEK-GIPR cells showed intense labeling of the plasma membrane immediately after addition of AlexaF647-GIP (Fig. 1A). Then, fluorescence was relocated in numerous membrane clusters and progressively penetrated into the cells as punctuate vesicles which formed clusters over the incubation time. Moreover, in HEKT293 transiently expressing GFP tagged GIPR, AlexaF647-GIP and GFP tagged GIPR co-localized during internalization and intracellular trafficking for at least 2 hours (Fig. 1B). This result establishes that internalized AlexaF647-GIP truly accounted for GIPR internalization. On the other hand, most of AlexaF647 and GFP fluorescence remained co-localized at time 5 hours, although some labeling appeared separately and GFP fluorescence intensity decreased likely because of degradation of GFP (Fig. 1B). Therefore, based on these controls and potential risks that GFP tag could hinder interactions between the intracellular region of GIPR and proteins of the endocytosis machinery, next experiments aimed at characterizing molecular mechanisms of GIPR internalization were carried out using AlexaF647-GIP to trace GIPR intracellular trafficking following internalization. It is worthy to mention that due to detection limits of confocal microscope and FACS, internalization and trafficking of the GIPR were investigated with concentrations of fluorescent probes equal or above 10 nM. Previous studies investigating GIPR targeting *in vivo* demonstrated GIPR internalization in response to picomolar concentrations of radio-labeled GIP [28].

Quantification of the amount of internalized ligand resistant to acid-washing which efficiently removed membrane-bound ligand (supplemental Fig. 2S) indicated that 60% and near 100% of bound AlexaF647-GIP became resistant to acid-washing after 5 and 30 min of incubation, respectively, demonstrating rapid and abundant trapping of GIPR in endocytosis structures (Fig. 1C).

3.2. Internalized GIP receptors poorly recycle and are mainly directed to lysosomes

The trafficking and fate of internalized GIPR was investigated in Flp-ln^{TM} HEK-GIPR. Results from experiments designed to examine possible recycling of internalized GIPR at the cell surface showed a slight increase of GIPR density through recycling which however did not exceed 10-15% of initial GIPR population after 1 hour (Fig. 2A). Trafficking was examined in Flp-ln^{TM} HEK transiently expressing both GFP tagged GIPR and fluorescent Rab proteins which are GTPases regulating intracellular trafficking between functionally distinct compartments in the cells [29]. Results showed early co-localization of internalized GIPR in Rab-5-positive early endosomes (Fig. 2B) and rare late co-localization in Rab-11 containing vesicles (Fig. 1C). On the other hand, transport to lysosomes was evaluated using LysoTracker, an acidic organelle-selective fluorescent probes. Confocal microscopy images indicate that a part of AlexaF647-GIP labeled GIPR and GIPR-GFP co-localized in lysoTracker-labeled lysosomes at 30 min and that almost the totality of internalized labeled GIP receptors were found in lysosomes at times 2 and 3 h (Fig. 2C).Together, these data demonstrate that GIPR receptors rapidly internalize upon GIP stimulation and are mostly directed to lysosomal degradation pathway, with only a minority of receptors recycling to the cell surface.

3.3. Internalization of GIP receptor involves clathrin-coated pits and dynamin

Internalization of GPCRs can occur through two main membrane structures, caveolae and clathrin-coated pits [21,30]. The role of clathrin in GIPR internalization was investigated by expressing a GFP tagged fragment of clathrin in the cells or by treating Flp-ln^{TM} HEK-GIPR cells with chlorpromazine, an inhibitor of clathrin-coated pit formation. As shown on Fig. 3A, in cells expressing GFP tagged fragment of clathrin, abundant punctuated co-localization with labeled GIPR was observed both at the cell surface and in endocytosis vesicles. Furthermore, Pitstop2 blocked AlexaF647- and GFP-labeled GIPR at the cell surface (Fig. 3B). Together, these results support that GIPR internalization occurred through clathrin-coated pits. The possibility that GIPR internalized through caveolae was also evaluated by expressing GFP tagged caveolin-1 in the cells or by treating Flp-ln^{TM} HEK-GIPR cells with filipin, a caveole inhibitor. GFP tagged caveolin-1 mostly remained at the cell membrane following stimulation with AlexaF647-GIP. Presence of GFP tagged caveolin-1 could be observed in some endocytosis vesicles containing AlexaF647-GIP (Supplemental Fig. 3S). On the other hand, the caveole inhibitor did not significantly affect GIPR internalization (Supplemental Fig. 3S). All together, these experiments support that internalization of GIPR likely occurs mainly through clathrin-coated pits in HEK cells.

The contribution of dynamin, a GTPase involved in the separation of endocytosis vesicles from the plasma membrane was assessed. As illustrated on Fig. 3C, in the presence dominant negative dynamin, DN-K44A, AlexaF 647-GIP labeled GIPR remained at the cell surface for a long period as labeled clusters and internalization was clearly delayed relative to control transfected cells. The delay of internalization was more pronounced in the presence of dynasore. Indeed, even after times of

incubation as long as 1h, most of the AlexaF647-labeled GIPR remained at the cell surface and a minority of labeled GIPR was internalized (Fig. 3C). These images clearly indicate that dynamin is required for the internalization of GIPR.

3.4. Internalization of the GIP receptor does not require β-arrestins nor C-terminal region of the receptor but involves AP-2

Most often, the cascade of molecular events in the process of GPCR internalization through clathrin-coated pits involves the phosphorylation by GRK of Ser/Thr residues located on extreme C-terminal region and/or intracellular loops of receptors and subsequent binding of β-arrestins which play a role of adaptor for receptor binding to both β2-subunit of AP-2 complex and clathrin [20].

The possible involvement of β-arrestins in GIPR internalization was examined. We first determined whether GIPR recruited β-arrestins using confocal microsopy and BRET, the later being recognized as a highly sensitive biophysical assay for detection of protein proximity [31]. Results showed no change in the concentration of cytoplasmic GFP tagged β-arrestin1 or 2 following GIP stimulations (Fig. 4A and supplemental Fig. 4S). In contrast, stimulation of CCK2R (used here as a receptor recruiting β-arrestins) caused rapid translocation of cytosolic GFP tagged β-arrestin1 or 2 to the cell plasma membrane upon activation. Moreover, no BRET signal between *R*Luc tagged GIPR and YFP tagged β-arrestin1 or 2 could be detected (illustrated only with YFP tagged β-arrestin2, Fig. 4S), whereas BRET signal was seen with CCK2R, as previously documented [32]. Absence of β-arrestin1/2 recruitment by GIPR was observed in confocal microscopy and BRET experiments with ratio of transfected plasmids ranging from 1:10 to 10:1. Collectively, these results indicate that GIPR most likely internalizes without requiring β-arrestin1 or 2 recruitment.

We then evaluated the involvement of the C-terminal region of GIPR by constructing truncated GIPR. The GIPR constructs were first tested for their ability to stimulate adenylyl cyclase in response to GIP. As shown on supplemental Fig. 5SA, truncated GIPR at residues 414, 432 or 452 responded to GIP stimulations by increasing cAMP levels to the same maximum as the wild-type GIPR. However, half-maximal stimulation of GIPR-TR414 or GIPR-TR432 required higher GIP concentrations than did the wild-type GIPR (EC_{50}: 5.2 ± 0.1 nM or 5.8 ± 0.1 nM versus 0.27 ± 0.21 nM, respectively) suggesting importance of the eliminated part of the receptor C-terminal tail for Gs coupling. Confocal microscopy observations indicate that abundant internalization could be seen in cells expressing the different truncated GIPR (Supplemental Fig. 5S, B). Quantification of internalization of these truncated GIPR using acid-washing showed no significant differences (Supplemental Fig. 5S, C). Therefore, none of the amino acids from C-terminal tail of GIPR seems to be essential for internalization, thus confirming previous data with rat GIPR [33].

Finally, the involvement of AP-2 in GIPR internalization was investigated by co-expressing YFP tagged β_2-subunit of AP-2 in Flp-ln^{TM} HEK-GIPR cells. Imaging results show abundant co-localization

between β_2-subunit of AP-2 and AlexaF647-labeled GIPR strongly suggesting participation of AP-2 complex to the internalization machinery of the GIPR (Fig. 4B).

3.5. N-acetylation of GIP affects activity of the peptide on cAMP production, GIPR internalization and GIPR desensitization

Structure-activity relationship data with GIP as well as mapping of GIP binding site in GIPR demonstrated that N-terminal region of GIP is essential for its biological activity [24,34,35]. On the other hand, N-terminal modifications of GIP were reported to increase resistance of GIP to degradation by DPP IV and/or its efficacy as an incretin [34,36]. We therefore tested whether N-acetyl modification of GIP affects ability of the peptide to trigger internalization and desensitization of the GIPR.

We first determined affinity of N-acetyl-GIP for human GIPR by performing binding experiments. Results show that N-acetyl-GIP competed with radio-iodinated GIP to GIPR with ~2.5-fold lower affinity than that of GIP (Ki : 28.6 ± 4.3 nM for N-acetyl GIP versus 11.3 ± 3.1 nM for GIP, supplemental Fig. 5A and table 1). On the other hand, N-acetyl-GIP stimulation of Flp-lnTM HEK-GIPR cells resulted in a dose-dependent increase of cAMP levels, with a maximal cAMP response close to that obtained with GIP, but a half-maximal response (EC_{50}) achieved with 14.8 ± 1.9 nM versus 1.1 ± 0.1 nM for GIP (Fig. 5B, supplemental table 1). Thus, N-acetyl-GIP behaved as a full agonist of the GIPR to stimulate cAMP formation in HEK 293 cells but was ~15-fold less potent that GIP.

Before use for internalization studies, AlexaF647-N-acetyl-GIP was characterized pharmacologically. Binding experiments indicated that AlexaF647-N-acetyl-GIP bound to GIPR with slightly lower affinity than that of unlabeled N-acetyl-GIP (Ki: 49.5 ± 5.8 versus 28.6 ± 4.3 nM, supplemental Fig. 6SA and table 1, supplemental data). Nevertheless, AlexaF647-N-acetyl-GIP stimulated cAMP production with a 15.5-fold lower potency than that of AlexaF647-GIP (EC_{50} : 7.3 ± 0.9 nM for AlexaF647-N-acetyl-GIP versus 0.47 ± 0.08 nM for AlexaF647-GIP, supplemental Fig. 6S and table 1), supporting again that N-acetyl moiety is more important for GIPR activation than for ligand binding.

Confocal microscopy studies of GIPR internalization following stimulation with 1 µM AlexaF647-N-acetyl-GIP showed minor internalization as compared with 0.1 µM AlexaF647-GIP which provided similar cAMP production levels (Fig. 5C). In agreement with this result, unlabeled N-acetyl-GIP did significantly stimulate internalization of GFP tagged GIPR transiently expressed in HEK 293T cells, thus ruling out a possible role of AlexaF647 moiety in the inability of N-acetyl-GIP to trigger GIPR internalization (Fig. 5C). Furthermore, using acid-washing procedure, we quantified internalization of GIPR in response to AlexaF647-N-acetyl-GIP in comparison to AlexaF647-GIP at times 5 and 30 min of stimulation. As illustrated on Fig. 6, after 5 min and 30 min of stimulation, the fraction of cell-associated AlexaF647-N-acetyl-GIP which remained resistant to acid-washing was significantly lower

than that of AlexaF647-GIP at the three concentrations tested. Despite no EC_{50} could be calculated because dose-response curves did not reach a plateau, data from acid-washing experiments support that AlexaF647-N-acetyl-GIP and AlexaF647-GIP stimulate differently trapping and/or internalization of the GIPR. Strikingly, between ~54 and ~75% of cell-associated AlexaF647-N-acetyl-GIP were resistant to acid-washing whereas only a minority of fluorescence was detected in the cell interior by confocal microscopy. This apparent discrepancy suggests that binding of AlexaF647-N-acetyl-GIP to GIPR was rapidly followed by its trapping (or sequestration) at the plasma membrane but this was not pursued by its complete internalization.

In light of the data showing distinct abilities of AlexaF647-N-acetyl-GIP and AlexaF647-GIP to stimulate GIPR internalization, we compared desensitization of cAMP responses stimulated with N-acetyl-GIP or GIP. Indeed, phosphorylation by second messenger-dependent protein kinases and G-protein-coupled receptor kinases (GRK) followed by internalization are major cause of desensitization of GPCR signaling [19,20]. For desensitization experiments, Flp-In™ HEK-GIPR cells were pre-stimulated with N-acetyl-GIP or GIP for different periods of time in order to cause desensitization of GIPR response. Then, cAMP production in response to a second agonist challenge was measured. As shown on Fig. 7, pre-stimulations with GIP dramatically decreased the ability of GIPR to respond to a second agonist challenge. Indeed, a 15-minute pre-stimulation decreased by 63% the cAMP response to GIP. In contrast, 15-minutes pre-stimulation of the cells with N-acetyl-GIP did not significantly affect cAMP responses; Neither GIP, nor N-acetyl-GIP pre-stimulation affected the ability of forskolin to increase cAMP level indicating that desensitization of cAMP responses was related to GIPR and not to adenylyl cyclase (not shown). Finally, PKA inhibitor, H89, which did not significantly affect internalization (Supplemental Fig. 7S) only partially reversed down regulation by GIP and entirely reversed N-acetyl-GIP-induced desensitization of cAMP response. In summary, N-acetyl-GIP differs from GIP mostly in its potency to stimulate cAMP production, as well as in its ability to desensitize GIPR-induced cAMP production and to stimulate GIPR internalization.

3.6. N-acetyl-GIP efficiently stimulates insulin secretion from MIN-6 cells.

We next compared stimulatory effects of GIP and N-acetyl-GIP on cultured β-cells. As shown on Fig. 8, both peptides dose-dependently stimulated insulin secretion. Insulin secretion levels with 1 and 10 nM as well as 0.1 µM N-acetyl-GIP were slightly (but not significantly) higher than that with GIP at equivalent concentrations. Unfortunately, the low number of GIPR receptors present at the cell surface of MIN-6 as well as the low level of insulin secretion did not allow us to investigate GIPR internalization and desensitization.

4. Discussion

In the context of a renewed interest for the development of GIP analogues therapeutic value, the aim of the current study was to investigate internalization of the GIPR following pharmacological stimulation by agonists, as well as the cellular and molecular underlying mechanisms. This study was carried out in HEK cells, a reference cell model for internalization studies.

By using two different means to trace GIPR internalization, namely fluorescent reversible labeling of the GIPR with AlexaF647-GIP or covalent labeling with the GFP tag, we show rapid and abundant internalization of the GIPR immediately after GIP stimulation. Once internalized, GIPR poorly recycles to the cell surface but rather co-localizes with LysoTracker labeled vesicles indicating major targeting to late endosomes and lysosomes. Furthermore, converging results obtained with chemical inhibitors (chlorpromazine or fillipin) and GFP tagged proteins (Lca clathrin-eYFP or caveolin1-GFP) of both clathrin-coated pits and caveolae clearly support that internalization of the GIPR occurs mainly through clathrin-coated pits, although we do not exclude that a minority of GIP-stimulated GIPR could internalize through caveolae. GIPR internalization was strongly diminished and delayed by a dominant-negative and a chemical inhibitor of dynamin, thus indicating involvement of this GTPase in the fission of GIPR-containing endocytosis vesicles from the cell plasma membrane.

The molecular events linking GIPR activation and its subsequent targeting to clathrin- coated pits were also investigated. Several lines of evidence support that GIPR internalization does not require β-arrestins. First, both confocal microscopy and BRET studies were unable to show recruitment of β-arrestin 1 or 2 whereas parallel experiments showed this recruitment to the CCK2R used as a reference receptor recruiting β-arrestins [32]. Moreover, elimination of phosphorylatable amino acids by truncation of C-terminal region of GIPR did not affect internalization of the GIPR, a result in agreement with previous reports by others showing that, although probably phosphorylated on two serines, the C-terminal tail of rodent GIPR was not essential for agonist-induced internalization [33,40]. Moreover, our results agree with those reported during the preparation of this manuscript, indicating no significant recruitment β-arrestin2 by the GIPR in HEK293 cells [41]. On the other hand, confocal microscopy observations strongly support participation of the AP-2 complex in GIPR internalization, a result in line with evidence showing that AP-2 is essential, if not required, in clathrin-coat pit formation [42,43]. β-arrestins are adaptor proteins classically recruited by phosphorylated G-protein coupled receptors, a biochemical event that is followed by binding of receptor-arrestin dimer to both β2-subunit of the AP-2 complex and clathrin, and subsequent targeting of the resulting cargo to clathrin-coated pits. The fact that GIPR internalization does not require β-arrestins whereas it involves AP-2 raises the question of the mechanism by which activated GIPR is targeted to AP-2 complex before endocytosis. In light of available data from the literature, several hypotheses can be proposed. First, activated GIPR might interact directly *via* intracytosolic endocytosis motifs with a subunit of AP-2 complex. Consensus endocytosis motifs capable to be recognized by AP-2 adaptor complex are YxxΦ tyrosine-based motifs where Φ can be F, I, L, M or V

as well as [ED]xxxL[LI] acidic dileucine motifs [21]. Several G-protein- coupled receptors, such as protease-activated receptor 1 (PAR1), the chemokine CXCR2 and CXCR4 receptors, and the β2-adrenergic receptor have been shown to internalize by involving such sorting motifs [44] [45-47]. We have performed an analysis of amino acid sequence of the GIPR and found 3 potential consensus sorting motifs in the intracytosolic region of the protein (bottom of transmembrane segments 2, 4 and 7). However, point-mutations within these motifs did not affect significantly GIPR internalization (unpublished data). Among other likely hypotheses, involvement of GPCR kinases (GRKs) is plausible. GRK are best known to phosphorylate intracellular domains of active GPCRs resulting in receptor desensitization and internalization and are also capable of regulating GPCR signaling and trafficking independently of phosphorylation [48-50]. GRK2 has been shown to directly interact with clathrin through a clathrin box [48-50]. However, contradictory results were reported about interaction of GRK2 with GIPR [40,41]. Indeed, recruitment assay using FRET could not detect any binding of GRK2 to the GIPR whereas GRK2 over-expression caused drops in GIPR-dependant cAMP production and insulin secretion [40,41].

An additional important finding of the current work is the identification of new pharmacological properties of N-acetyl-GIP. This peptide was previously shown to have an improved anti-hyperglycemic activity and stimulatory action on insulin secretion *in vivo* in ob/ob mice [51]. The half-life of N-acetyl-GIP to DPP IV degradation was estimated to be >24 hours in plasma versus 6.2 hours for natural GIP [52]. In the current study, N-acetyl-GIP was found to be as potent and efficient as GIP to stimulate insulin secretion from MIN-6-B1 cells in spite of its 15-fold lower potency to stimulate cAMP production. These findings must be examined in light of results showing that N-acetyl-GIP incompletely stimulates GIPR endocytosis and displays a decreased ability to desensitize GIP-induced cAMP production. It is thus plausible that N-acetylation of GIP improves insulinotropic action of the peptide by decreasing its potency to stimulate desensitization, internalization and lysosomal degradation of the GIPR. Additionally, like several other G-protein coupled receptors, GIPR might stimulate cAMP production from plasma membrane and early endocytosis vesicles as well and both cAMP pools would contribute to insulin secretion [53]. Related to this hypothesis, it will be important to investigate precise early trafficking of GIPR stimulated both by GIP and N-acetyl-GIP, as well as possible differential effects of the two peptides on GIPR recycling.

Thus, N-acetylation has a minor impact on affinity of GIP for its receptor but more strongly affects ability of GIP to activate GIPR. These findings are compatible with converging data showing that N-terminal part of GIP is crucial for activation of the GIPR, whereas the C-terminal region of GIP is essentially involved in ligand binding [24,34,35,37]. Also, our previous studies dedicated to mapping of the activation site of the GIPR showed that N-terminus of receptor-bound GIP is in contact with aminoacids from transmembrane domains of the GIPR [24]. Our results showing distinct behaviors of N-acetyl-GIP relative to the full agonist GIP led us to examine if this could be explained by different binding poses of the two ligands in the binding site of the modeled GIPR. We previously identified

amino acid residues of the GIPR binding site that are essential for GIPR activation by GIP using an iterative approach involving homology modeling based on templates of Group A GPCRs and site-directed mutagenesis [24]. For the purpose of this study, we have validated the data by reconstructing the GIPR homology model using the recently published crystal structure of the human glucagon receptor (GCGR), a Group B GPCR having a sequence identity of 58% with GIPR. In the modeled GIPR.GIP complex represented in Fig. 9A and B, the side chain of Tyr1 in GIP forms a H-bond with Q224 and a cation-π interaction with R300 and the terminal ammonium moiety of Tyr1 has an ionic interaction with E377 and a cation-π interaction with F357. The side chain of Glu3 forms an ionic interaction with R183. The backbone of Gly4 forms a H-bond with R190. The importance of R183, R190, Q224, R300 and F357 in GIPR activation by GIP agrees with earlier site-directed mutagenesis results [24]. Docking of N-acetyl-GIP in the binding site of the GIPR indicates that N-acetyl-GIP maintains the most of contacts apart from interactions with E377 and F357, acetylated nitrogen being moved away from these residues (Fig. 9C). As a consequence, N-acetyl-GIP has a less number of interactions with helices 6 and 7 compared to GIP. These results, together with data showing that helices 6 and 7 in G-protein coupled receptors are essential for stabilization of the active conformation of receptors, may explain atypical activity of N-acetyl-GIP analogue [37-39]. So, it is plausible that the two agonists may stabilize different conformations of the GIPR, each of which having distinct ability to trigger signals.

The understanding of the origin of incomplete internalization and decreased desensitization of GIPR following stimulation by N-acetyl-GIP will deserve additional investigations. Meanwhile, the fact that the PKA inhibitor fully reverses desensitization by N-acetyl-GIP whereas it partly reverses that by GIP supports the view that distinct signaling pathways and mechanisms cause desensitization of GIPR response: weak desensitization following N-acetyl-GIP exposure would mainly involve cAMP-dependent protein kinase (PKA) whereas more intensive desensitization by GIP would involve both PKA and other signaling pathways, including those leading to internalization. Thus, it is plausible that N-acetyl-GIP fails to activate a step of GIPR signaling involved in both desensitization and internalization. Accordingly, N-acetyl-GIP is a biased agonist candidate.

Our results on GIPR internalization in HEK cells differ from those recently reported in transfected 3T3L1 adipocytes [18]. In the last study, it was shown that GIPR constitutively internalizes and recycles to the cell surface and GIP regulates down-regulation of plasma membrane GIPR by slowing GIPR recycling without affecting kinetics of GIPR internalization [18]. We have no explanation for such different findings excepted that GIPR, like other G-protein coupled receptors, could behave differently according to the cell context [54]. On the other hand, it is interesting to compare behavior of the GIPR with that of the GLP1R. Indeed, although these two receptors are highly homologous in structure and functions, their insulinotropic responses are differently affected in diabetics. Studies insulinoma and HEK cells both showed that GLP1 rapidly internalizes in response to its natural agonist but also rapidly recycles to the cell surface [55,56]. Furthermore, GLP1 was shown to recruit

GRK2 and β-arrestin2 upon activation [41]. Thus, with respect to recycling to the cell surface and molecular mechanisms involved in internalization, GIPR seems to differ from GLP-1R [41,55,56].

5. Conclusion

In this study, internalization of the GIPR and subsequent intracellular trafficking has been characterized. GIP stimulated rapid robust internalization of the GIPR, the major part being directed to lysosomes. GIPR internalization involved clathrin-coated pits, AP-2 and dynamin. However, neither GIPR C-terminal region nor β-arrestin1/2 was required. Thus, mechanisms of GIPR internalization seems to differ from that reported for GLP1R. Finally, N-acetyl-GIP recognized as a dipeptidyl-IV resistant analogue appeared to weakly stimulate GIPR internalization and desensitization of cAMP response. Molecular modelingof GIPR.N-acetyl-GIP complex enabled to show that N-acetyl-GIP interact more slightly with amino acids of helices 6 and 7 of the GIPR compared to GIP, supporting that the two agonists may stabilize different conformations of the GIPR, each of which having distinct ability to trigger signals. We propose that incomplete or partial activity of N-acetyl-GIP on signaling involved in GIPR desensitization and internalization contributes to the enhanced incretin activity of this peptide which is a biased agonist candidate.

6. Acknowledgements

We greatly appreciate the gifts of plasmids encoding YFP tagged β -arrestin-2, from Marc Caron (Duke University Medical Center, Durham, USA), GFP tagged β-arrestin-2 from Robert Lefkowitz (Duke University Medical Center, Durham) and YFP tagged β-adaptin2 from Michel Bouvier (Montreal university, Canada). We thank Bernard Masri for his helpful advices in BRET experiments and Laurie Sarrat for her technical assistance.

7. Footnotes

Sadek Ismail and Ingrid Dubois-Vedrenne equally contributed to the work. The work was supported by a Grant number 10009090 from Region Midi-Pyrénées.

8. References:

[1] Jornvall, H., Carlquist, M., Kwauk, S., Otte, S.C., McIntosh, C.H., Brown, J.C. and Mutt, V. (1981) Amino acid sequence and heterogeneity of gastric inhibitory polypeptide (GIP). FEBS Lett 123, 205-10.

[2] Moody, A.J., Thim, L. and Valverde, I. (1984) The isolation and sequencing of human gastric inhibitory peptide (GIP). FEBS Lett 172, 142-8.

[3] Baggio, L.L. and Drucker, D.J. (2007) Biology of incretins: GLP-1 and GIP. Gastroenterology 132, 2131-57.

[4] Gremlich, S., Porret, A., Hani, E.H., Cherif, D., Vionnet, N., Froguel, P. and Thorens, B. (1995) Cloning, functional expression, and chromosomal localization of the human pancreatic islet glucose-dependent insulinotropic polypeptide receptor. Diabetes 44, 1202-8.

[5] Bockaert, J. and Pin, J.P. (1999) Molecular tinkering of G protein-coupled receptors: an evolutionary success. EMBO J 18, 1723-9.

[6] Nauck, M.A., Heimesaat, M.M., Orskov, C., Holst, J.J., Ebert, R. and Creutzfeldt, W. (1993) Preserved incretin activity of glucagon-like peptide 1 [7-36 amide] but not of synthetic human gastric inhibitory polypeptide in patients with type-2 diabetes mellitus. J Clin Invest 91, 301-7.

[7] Younan, S.M. and Rashed, L.A. (2007) Impairment of the insulinotropic effect of gastric inhibitory polypeptide (GIP) in obese and diabetic rats is related to the down-regulation of its pancreatic receptors. Gen Physiol Biophys 26, 181-93.

[8] Kieffer, T.J., McIntosh, C.H. and Pederson, R.A. (1995) Degradation of glucose-dependent insulinotropic polypeptide and truncated glucagon-like peptide 1 in vitro and in vivo by dipeptidyl peptidase IV. Endocrinology 136, 3585-96.

[9] Vilsboll, T., Krarup, T., Madsbad, S. and Holst, J.J. (2002) Defective amplification of the late phase insulin response to glucose by GIP in obese Type II diabetic patients. Diabetologia 45, 1111-9.

[10] Lynn, F.C., Pamir, N., Ng, E.H., McIntosh, C.H., Kieffer, T.J. and Pederson, R.A. (2001) Defective glucose-dependent insulinotropic polypeptide receptor expression in diabetic fatty Zucker rats. Diabetes 50, 1004-11.

[11] Piteau, S., Olver, A., Kim, S.J., Winter, K., Pospisilik, J.A., Lynn, F., Manhart, S., Demuth, H.U., Speck, M., Pederson, R.A. and McIntosh, C.H. (2007) Reversal of islet GIP receptor down-regulation and resistance to GIP by reducing hyperglycemia in the Zucker rat. Biochem Biophys Res Commun 362, 1007-12.

[12] Hojberg, P.V., Vilsboll, T., Rabol, R., Knop, F.K., Bache, M., Krarup, T., Holst, J.J. and Madsbad, S. (2009) Four weeks of near-normalisation of blood glucose improves the insulin response to glucagon-like peptide-1 and glucose-dependent insulinotropic polypeptide in patients with type 2 diabetes. Diabetologia 52, 199-207.

[13] Finan, B., Ma, T., Ottaway, N., Muller, T.D., Habegger, K.M., Heppner, K.M., Kirchner, H., Holland, J., Hembree, J., Raver, C., Lockie, S.H., Smiley, D.L., Gelfanov, V., Yang, B., Hofmann, S., Bruemmer, D., Drucker, D.J., Pfluger, P.T., Perez-Tilve, D., Gidda, J., Vignati, L., Zhang, L., Hauptman, J.B., Lau, M., Brecheisen, M., Uhles, S., Riboulet, W., Hainaut, E., Sebokova, E., Conde-Knape, K., Konkar, A., Dimarchi, R.D. and Tschop, M.H. (2013) Unimolecular dual incretins maximize metabolic benefits in rodents, monkeys, and humans. Sci Transl Med 5, 209ra151.

[14] Irwin, N., Gault, V. and Flatt, P.R. (2010) Therapeutic potential of the original incretin hormone glucose-dependent insulinotropic polypeptide: diabetes, obesity, osteoporosis and Alzheimer's disease? Expert Opin Investig Drugs 19, 1039-48.

[15] Tatarkiewicz, K., Hargrove, D.M., Jodka, C.M., Gedulin, B.R., Smith, P.A., Hoyt, J.A., Lwin, A., Collins, L., Mamedova, L., Levy, O.E., D'Souza, L., Janssen, S., Srivastava, V., Ghosh, S.S. and Parkes, D.G. (2013) A novel long-acting glucose-dependent insulinotropic peptide analogue: enhanced efficacy in normal and diabetic rodents. Diabetes Obes Metab.

[16] Tseng, C.C., Boylan, M.O., Jarboe, L.A., Usdin, T.B. and Wolfe, M.M. (1996) Chronic desensitization of the glucose-dependent insulinotropic polypeptide receptor in diabetic rats. Am J Physiol 270, E661-6.

[17] Hinke, S.A., Pauly, R.P., Ehses, J., Kerridge, P., Demuth, H.U., McIntosh, C.H. and Pederson, R.A. (2000) Role of glucose in chronic desensitization of isolated rat islets and mouse insulinoma (betaTC-3) cells to glucose-dependent insulinotropic polypeptide. J Endocrinol 165, 281-91.

[18] Mohammad, S., Patel, R.T., Bruno, J., Panhwar, M.S., Wen, J. and McGraw, T.E. (2014) A naturally occurring GIP receptor variant undergoes enhanced agonist-induced desensitization, which impairs GIP control of adipose insulin sensitivity. Mol Cell Biol 34, 3618-29.

[19] Marchese, A., Paing, M.M., Temple, B.R. and Trejo, J. (2008) G protein-coupled receptor sorting to endosomes and lysosomes. Annu Rev Pharmacol Toxicol 48, 601-29.

[20] Ferguson, S.S. (2001) Evolving concepts in G protein-coupled receptor endocytosis: the role in receptor desensitization and signaling. Pharmacol Rev 53, 1-24.

[21] Traub, L.M. (2009) Tickets to ride: selecting cargo for clathrin-regulated internalization. Nat Rev Mol Cell Biol 10, 583-96.

[22] Sorkin, A. and von Zastrow, M. (2009) Endocytosis and signalling: intertwining molecular networks. Nat Rev Mol Cell Biol 10, 609-22.

[23] Rajagopal, S., Rajagopal, K. and Lefkowitz, R.J. (2010) Teaching old receptors new tricks: biasing seven-transmembrane receptors. Nat Rev Drug Discov 9, 373-86.

[24] Yaqub, T., Tikhonova, I.G., Lattig, J., Magnan, R., Laval, M., Escrieut, C., Boulegue, C., Hewage, C. and Fourmy, D. (2010) Identification of determinants of glucose-dependent insulinotropic polypeptide receptor that interact with N-terminal biologically active region of the natural ligand. Mol Pharmacol 77, 547-58.

[25] Foucaud, M., Marco, E., Escrieut, C., Low, C., Kalindjian, B. and Fourmy, D. (2008) Linking non-peptide ligand binding mode to activity at the human cholecystokinin-2 receptor. J Biol Chem 283, 35860-8.

[26] Siu, F.Y., He, M., de Graaf, C., Han, G.W., Yang, D., Zhang, Z., Zhou, C., Xu, Q., Wacker, D., Joseph, J.S., Liu, W., Lau, J., Cherezov, V., Katritch, V., Wang, M.W. and Stevens, R.C.

(2013) Structure of the human glucagon class B G-protein-coupled receptor. Nature 499, 444-9.

[27] Parthier, C., Kleinschmidt, M., Neumann, P., Rudolph, R., Manhart, S., Schlenzig, D., Fanghanel, J., Rahfeld, J.U., Demuth, H.U. and Stubbs, M.T. (2007) Crystal structure of the incretin-bound extracellular domain of a G protein-coupled receptor. Proc Natl Acad Sci U S A 104, 13942-7.

[28] Gourni, E., Waser, B., Clerc, P., Fourmy, D., Reubi, J.C. and Maecke, H.R. (2014) The Glucose-Dependent Insulinotropic Polypeptide Receptor: A Novel Target for Neuroendocrine Tumor Imaging-First Preclinical Studies. J Nucl Med 55, 976-982.

[29] Stenmark, H. (2009) Rab GTPases as coordinators of vesicle traffic. Nat Rev Mol Cell Biol 10, 513-25.

[30] Mayor, S. and Pagano, R.E. (2007) Pathways of clathrin-independent endocytosis. Nat Rev Mol Cell Biol 8, 603-12.

[31] Hamdan, F.F., Percherancier, Y., Breton, B. and Bouvier, M. (2006) Monitoring protein-protein interactions in living cells by bioluminescence resonance energy transfer (BRET). Curr Protoc Neurosci Chapter 5, Unit 5 23.

[32] Magnan, R., Masri, B., Escrieut, C., Foucaud, M., Cordelier, P. and Fourmy, D. (2011) Regulation of membrane cholecystokinin-2 receptor by agonists enables classification of partial agonists as biased agonists. J Biol Chem 286, 6707-19.

[33] Wheeler, M.B., Gelling, R.W., Hinke, S.A., Tu, B., Pederson, R.A., Lynn, F., Ehses, J. and McIntosh, C.H. (1999) Characterization of the carboxyl-terminal domain of the rat glucose-dependent insulinotropic polypeptide (GIP) receptor. A role for serines 426 and 427 in regulating the rate of internalization. J Biol Chem 274, 24593-601.

[34] Gault, V.A., Flatt, P.R. and O'Harte, F.P. (2003) Glucose-dependent insulinotropic polypeptide analogues and their therapeutic potential for the treatment of obesity-diabetes. Biochem Biophys Res Commun 308, 207-13.

[35] Hinke, S.A., Manhart, S., Pamir, N., Demuth, H., R, W.G., Pederson, R.A. and McIntosh, C.H. (2001) Identification of a bioactive domain in the amino-terminus of glucose-dependent insulinotropic polypeptide (GIP). Biochim Biophys Acta 1547, 143-55.

[36] Irwin, N., Green, B.D., Mooney, M.H., Greer, B., Harriott, P., Bailey, C.J., Gault, V.A., O'Harte, F.P. and Flatt, P.R. (2005) A novel, long-acting agonist of glucose-dependent insulinotropic polypeptide suitable for once-daily administration in type 2 diabetes. J Pharmacol Exp Ther 314, 1187-94.

[37] Hollenstein, K., de Graaf, C., Bortolato, A., Wang, M.W., Marshall, F.H. and Stevens, R.C. (2014) Insights into the structure of class B GPCRs. Trends Pharmacol Sci 35, 12-22.

[38] Audet, M. and Bouvier, M. (2012) Restructuring G-protein- coupled receptor activation. Cell 151, 14-23.

[39] Magnan, R., Escrieut, C., Gigoux, V., De, K., Clerc, P., Niu, F., Azema, J., Masri, B., Cordomi, A., Baltas, M., Tikhonova, I.G. and Fourmy, D. (2013) Distinct CCK-2 receptor conformations associated with beta-arrestin-2 recruitment or phospholipase-C activation revealed by a biased antagonist. J Am Chem Soc 135, 2560-73.

[40] Tseng, C.C. and Zhang, X.Y. (2000) Role of G protein-coupled receptor kinases in glucose-dependent insulinotropic polypeptide receptor signaling. Endocrinology 141, 947-52.

[41] Al-Sabah, S., Al-Fulaij, M., Shaaban, G., Ahmed, H.A., Mann, R.J., Donnelly, D., Bunemann, M. and Krasel, C. (2014) The GIP receptor displays higher basal activity than the GLP-1 receptor but does not recruit GRK2 or arrestin3 effectively. PLoS One 9, e106890.

[42] Boucrot, E., Saffarian, S., Zhang, R. and Kirchhausen, T. Roles of AP-2 in clathrin-mediated endocytosis. PLoS One 5, e10597.

[43] Motley, A., Bright, N.A., Seaman, M.N. and Robinson, M.S. (2003) Clathrin-mediated endocytosis in AP-2-depleted cells. J Cell Biol 162, 909-18.

[44] Paing, M.M., Johnston, C.A., Siderovski, D.P. and Trejo, J. (2006) Clathrin adaptor AP2 regulates thrombin receptor constitutive internalization and endothelial cell resensitization. Mol Cell Biol 26, 3231-42.

[45] Fan, G.H., Yang, W., Wang, X.J., Qian, Q. and Richmond, A. (2001) Identification of a motif in the carboxyl terminus of CXCR2 that is involved in adaptin 2 binding and receptor internalization. Biochemistry 40, 791-800.

[46] Orsini, M.J., Parent, J.L., Mundell, S.J., Marchese, A. and Benovic, J.L. (2000) Trafficking of the HIV coreceptor CXCR4: role of arrestins and identification of residues in the C-terminal tail that mediate receptor internalization. J Biol Chem 275, 25876.

[47] Gabilondo, A.M., Hegler, J., Krasel, C., Boivin-Jahns, V., Hein, L. and Lohse, M.J. (1997) A dileucine motif in the C terminus of the beta2-adrenergic receptor is involved in receptor internalization. Proc Natl Acad Sci U S A 94, 12285-90.

[48] Pals-Rylaarsdam, R., Xu, Y., Witt-Enderby, P., Benovic, J.L. and Hosey, M.M. (1995) Desensitization and internalization of the m2 muscarinic acetylcholine receptor are directed by independent mechanisms. J Biol Chem 270, 29004-11.

[49] Moore, C.A., Milano, S.K. and Benovic, J.L. (2007) Regulation of receptor trafficking by GRKs and arrestins. Annu Rev Physiol 69, 451-82.

[50] Shiina, T., Arai, K., Tanabe, S., Yoshida, N., Haga, T., Nagao, T. and Kurose, H. (2001) Clathrin box in G protein-coupled receptor kinase 2. J Biol Chem 276, 33019-26.

[51] O'Harte, F.P., Gault, V.A., Parker, J.C., Harriott, P., Mooney, M.H., Bailey, C.J. and Flatt, P.R. (2002) Improved stability, insulin-releasing activity and antidiabetic potential of two novel N-terminal analogues of gastric inhibitory polypeptide: N-acetyl-GIP and pGlu-GIP. Diabetologia 45, 1281-91.

[52] Gault, V.A., O'Harte, F.P. and Flatt, P.R. (2003) Glucose-dependent insulinotropic polypeptide (GIP): anti-diabetic and anti-obesity potential? Neuropeptides 37, 253-63.

[53] Calebiro, D., Nikolaev, V.O., Persani, L. and Lohse, M.J. (2010) Signaling by internalized G-protein-coupled receptors. Trends Pharmacol Sci 31, 221-8.

[54] Tobin, A.B., Butcher, A.J. and Kong, K.C. (2008) Location, location, location...site-specific GPCR phosphorylation offers a mechanism for cell-type-specific signalling. Trends Pharmacol Sci 29, 413-20.

[55] Widmann, C., Dolci, W. and Thorens, B. (1995) Agonist-induced internalization and recycling of the glucagon-like peptide-1 receptor in transfected fibroblasts and in insulinomas. Biochem J 310 (Pt 1), 203-14.

[56] Roed, S.N., Wismann, P., Underwood, C.R., Kulahin, N., Iversen, H., Cappelen, K.A., Schaffer, L., Lehtonen, J., Hecksher-Soerensen, J., Secher, A., Mathiesen, J.M., Brauner-Osborne, H., Whistler, J.L., Knudsen, S.M. and Waldhoer, M. (2013) Real-time trafficking and signaling of the glucagon-like peptide-1 receptor. Mol Cell Endocrinol.

9. **Legends to Figures:**

Fig. 1: internalization of human GIP receptor

A: GIPR internalization was traced using AlexaF647-GIP (≈100 nM) incubated for indicated times with Flp-InTM HEK-GIPR cells. Images show a cell representative of the population in a single experiment. Cells expressing lower levels of GIPR (as shown by AlexaF647-GIP binding) presented an identical profile of internalization.

B: GIPR internalization was traced using GFP-tagged GIP receptor. HEK 293T cells transiently expressing GFP-tagged GIP (green) were incubated with AlexaF647-GIP (100 nM, red) for indicated times. Merged confocal microscopy images show AlexaF647-GIP co-localization with GFP tagged GIPR during intracellular trafficking. Images at different times correspond to distinct field from the same cell population.

C: Quantification of GIPR internalization. AlexaF647-GIP (≈100 nM) was incubated with Flp-In^{TM} HEK-GIPR cells for indicated times. Cells were directly assayed for fluorescence by FACS to measure amount of both bound and internalized AlexaF647-GIP (black bars) or were acid-washed before measuring cell-associated fluorescence (white bars), which according to confocal experiment control (Fig. 2S), corresponded to GIPR-mediated trapped and internalized AlexaF647-GIP. Values are expressed as % of maximum fluorescent labeling and are mean ± SEM of 3 experiments. Statistical significance of resistant acid-washing uptake versus total uptake: * $0.01<p<0.05$.

Fig. 2: Analysis of recycling and trafficking of internalized human GIP receptor

A: Graph shows results from quantification of GIPR recycling. Cells were treated with GIP (100 nM) for 1 hour, washed several times and incubated without ligand for indicated times to enable GIPR recycling at the cell surface. Then, cells were incubated with AlexaF647-GIP (1 µM) for 45 min and presence of GIPR was assayed using FACS. Values are the mean ± SEM of at least 3 separate experiments. The value 100 corresponds to cell-associated fluorescence at time 0 of recycling. Statistical significance of recycling values in reference to initial value: * $0.01<p<0.05$; ** $0.001<p<0.01$; *** $p<0.001$.

B1 and B2: Intracellular trafficking was traced by co-transfecting HEK 293T cells with cDNA encoding GIPR or GIPR-GFP and Rab5-DsRed or Rab11-DsRed. Images were captured at times 3, 6 and 24 min in B1, and at 4h in B2 after stimulation by AlexaF647-GIP (100 nM). Images in B1 show examples of co-localization of AlexaF647-GIP labeled GIPR (in red) with Rab5-DsRed (in green) in early endosomes at initial steps of trafficking (3-24 min). Images B2 show rare triple co-localization between AlexaF647-GIP (shown in red), GIPR-GFP (shown in blue) and Rab11-DsRed in slow

recycling endosomes at long times of incubation (between 2 and 5.5 h, illustrated for time 4h). These images are representative of 3 microcopy fields from 2 distinct experiments.

C: Flp-In™ HEK cells transfected with GFP-tagged GIP receptor were incubated with LysoTracker (75 nM, displayed in green) for 15 min. AlexaF647-GIP (100 nM) was added to the cells and incubated for 30 min. At this time, incubation medium was withdrawn, cells were washed once with PBS and new buffer without AlexaF647-GIP was added. Trafficking of internalized GIPR was let to proceed at 37°C. Images show that only a part of AlexaF647-GIP labeled GIPR (shown in red) and GIPR-GFP (shown in blue) co-localized in lysoTracker-labeled lysosomes at 30 min (shown in green, the arrow indicates an example of absence of co-localization). Co-localization in lysosomes increased over the time of incubation, as displayed at 2h and 3h. These images are representative of 4-5 microcopy fields from 2 distinct experiments.

Fig. 3: Human GIP receptor internalization involves clathrin coated-pits and dynamin

A: HEK 293T cells co-transfected with cDNA encoding GIPR and Clathrin-LCa-eYFP were stimulated with AlexaF647-GIP for indicated times. Merge images show co-localization of eYFP-tagged chlathin with AlexaF647-labeled GIPR both at the cell surface and in endocytosis vesicles. Images at different times correspond to different microcopy fields representative of several others.

B: HEK 293 cells transfected with cDNA encoding GIPR-GFP were incubated with AlexaF647-GIP alone or in the presence of the clathrin inhibitor, Pitstop2 (25µM). For each condition, images correspond to a single microscopy field representative of 2 others. They show that AlexaF647-labeled GIPR-GFP is maintained at the cell surface in the presence of Pitstop2. It was observed that Pitstop2 decreased intensity of AlexaF647 fluorescence over the time. Therefore, in order to ensure visualization of the GIPR, the experiment was performed on cells expressing GIPR-GFP and not on Flp-In™ HEK-GIPR cells.

C: Flp-In™ HEK-GIPR cells were incubated with AlexaF647-GIP alone (left panels) or HEK 293T cells co-transfected with cDNA encoding GIPR and dominant negative DN-K44A of dynamin were stimulated with AlexaF647-GIP for indicated times (midle panels) or Flp-In™ HEK-GIPR cells were incubated with AlexaF647-GIP in the presence of dynasore (50 µM) (right panels). Images showing different microscopy fields representative of several others indicate that both the dominant negative of dynamin and the chemical inhibitor strongly delay the process of GIPR internalization.

Fig. 4: Human GIP receptor internalization involves AP-2 complex and does not require β-arrestins

A: Flp-In™ HEK-GIPR cells or Flp-In™ HEK-CCK2R transfected with β-arrestin2-GFP were stimulated with GIP or CCK (100 nM), respectively. Images show that β-arrestin2-GFP remains in the cytoplasm in stimulated Flp-In™ HEK-GIPR cells whereas it was translocated to the plasma membrane (shown at time 5 min) in stimulated Flp-InTM HEK-CCK2R cells used as positive control of β-arrestin2 recruitment. Graphs of recruitment assay represent measurement of cytosolic fluorescence over the time after GIP or CCK stimulation. They show that cytosolic β-arrestin2-GFP concentration remains unchanged in stimulated Flp-In™ HEK-GIPR cells whereas it rapidly decreases in stimulated Flp-In™ HEK-CCK2R cells.

B: HEK293 T cells co-transfected with wild-type GIPR and YFP tagged β2-subunit of AP-2 were stimulated with AlexaF647-GIP (100 nM). Confocal microscopy Images show co-localization of AlexaF647-GIP labeled GIPR with YFP tagged β2-subunit of AP-2 on plasma membrane as well in endocytosis vesicles (shown at times 30 and 60 min.)

Fig. 5: N-acetylation of GIP affects activity of the peptide on cAMP production and GIPR internalization in HEK cells.

A: Inhibition of ^{125}I-Phe1-GIP binding by GIP or N-acetyl GIP to GIP receptor. Flp-In™ HEK-GIPR cells were incubated with ^{125}I-Phe1-GIP (100 pM) alone or in the presence of increasing concentrations of GIP or N-acetyl-GIP for 30 min. Bound radio-ligand was assayed and expressed as percent of specific binding. Results are mean ± SEM of 4 individual experiments. Inhibition constants, Ki, were: 11.3 ± 3.1 nM for GIP and 28.6 ± 4.3 nM for N-acetyl-GIP. These were significantly significant, $p<0.05$.

B: Dose-response curves of cAMP production in Flp-In™ HEK-GIPR stimulated with GIP or N-acetyl-GIP. cAMP levels were measured by BRET as described in the section "Materials and methods". cAMP levels with each concentration of agonist were expressed as percent of cAMP level achieved with 10µM GIP. Results are mean ± SD of 4 individual experiments. Concentration giving half-maximal responses were 1.1 ± 0.1 nM and 14.8 ± 1.9 nM, respectively. These were significantly significant, $p<0.001$.

C: Flp-In™ HEK-GIPR cells were stimulated by AlexaF647-GIP or AlexaF647-N-acetyl-GIP at 0.1 and 1µM, respectively. Images show absence of intemalization of AlexaF647-N-acetyl-GIP labeled GIPR (midle panels). HEK293 T cells were transfected with GIPR-GFP and stimulated with N-acetyl-GIP. Images (right panels) confirm that GIPR-GFP remains at the cell surface. Positive control of internalization of GIPR-GFP following GIP stimulation is shown on Fig. 1. Each kinetic is shown for the same microscope field. Images are those from an experiment representative of at least two others.

Fig. 6: Quantification of uptake of AlexaF647-GIP or AlexaF647-N-acetyl-GIP by HEK cells expressing GIP receptors.

Flp-In™ HEK-GIPR cells were incubated at 37°C with AlexaF647-GIP or AlexaF647-N-acetyl-GIP at different concentrations. At time 5 and 30 min, cells were directly assayed for fluorescence by FACS to measure amount of both bound and internalized AlexaF647-GIP (**panel A**) or were acid-washed before measuring cell-associated fluorescence (**panel B**). Histograms **A** represent mean ± SEM of total cell-associated fluorescence from 3 separated experiments, and histograms **B** represent the percent of cell-associated fluorescence resistant to acid-washing. Percent of cell-associated AlexaF647-N-acetyl-GIP resistant to acid washing was compared to that of cell-associated AlexaF647-GIP resistant to acid washing. Significance was as follows: ** $0.001<p<0.01$; ***$p<0.001$.

Fig. 7: Differential desensitization of GIPR-dependant cAMP production by GIP and N-acetyl-GIP.

HEK 293T cells co-transfected with cDNA encoding GIPR and EPAC Bret sensor were pre-stimulated with GIP (0.1µM) or N-acetyl-GIP (1µM) for indicated times. Then, cells were washed and stimulated with GIP (0.1µM) or N-acetyl-GIP (1µM) alone or in the presence PKA inhibitor, H89. cAMP production was determined by BRET measurements as described in "Materials and methods" section. Significance for cAMP production of cells pre-stimulated with GIP and N-acetyl-GIP without H89 is given in comparison with corresponding untreated cells. * $0.01<p<0.05$; ** $0.001<p<0.01$; Significance is also shown for cAMP in the presence of H89 as compared to cAMP in the absence of H89, • $0.01<p<0.05$; •• $0.001<p<0.01$. Results indicate that GIP-induced down regulation of cAMP production was more pronounced and observed earlier than that with N-acetyl-GIP. Moreover, H89 only reversed a fraction of GIP-induced desensitization of cAMP production whereas it fully reversed N-acetyl-GIP-induced desensitization of cAMP production.

Fig. 8: N-acetyl-GIP and GIP stimulations of insulin secretion from MIN-6-B1 cells.

Insulinoma cells (3.10^5cells/well) were grown in 24-wells plates for 48h. After washing, cells were incubated for 2h at 37°C in KRH buffer supplemented with 2.8 mM glucose. The incubation medium was discarded and replaced with 500 µL buffer containing 11 mM glucose with or without human GIP or N-acetyl-GIP. Cells were let to secrete insulin during 2h. Insulin secreted in supernatants was assayed by Elisa and results were expressed as -fold basal value obtained in the absence of peptide. Results are the mean ± SEM of 4 individual experiments.

Fig. 9: Molecular models of GIP and N-acetyl-GIP binding at GIPR.

A: Overall view of GIPR in the complex with GIP. B: Zoomed view of the GIP binding site. C: Zoomed view of the acylGIP binding site. Unlike GIP, N-acetyl-GIP does not form an ionic interaction with E377 and a cation-π interaction with F357. Only the first five residues of GIP and residues of the helical bundle predicted to be important for GIPR activation based on previous site-directed mutagenesis are shown in stick-like representation. Hydrogen bonds and π-cation interactions are in pink and dark green, respectively.

	GIP	N-acetyl-GIP	AlexaF647-GIP	AlexaF647-N-acetyl-GIP
cAMP (EC_{50} ± SEM, nM)	**1.1 ± 0.2**	**14.8 ± 1.9 ***(a)**	**0.47 ± 0.10**	**7.3 ± 0.9 ✸✸(b)**
Binding (Ki ± SEM, nM)	**11.3 ± 3.1**	**28.6 ± 4.3*(c)**	**25.5 ± 5.7**	**49.5 ± 5.8 ✸(d)**

Table 1: Summary of the pharmacological parameters of GIPR ligands

(a) and (c): comparison EC_{50} and Ki of N-acetyl-GIP versus EC_{50} and Ki of GIP

***p<0.001; * 0.01<p<0.05.

(b) and (d): comparison EC_{50} and Ki of AlexaF647-N-acetyl-GIP versus EC_{50} and Ki of AlexaF647-GIP; ✸✸ 0.001<p<0.01; ✸ 0.01<p<0.05.

A: AlexaF647-GIP

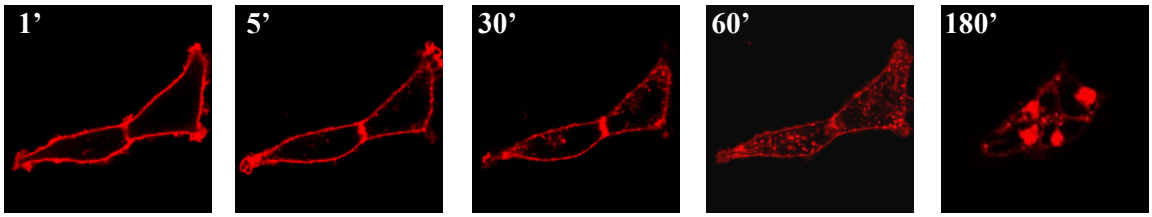

B: AlexaF647-GIP GIPR-GFP

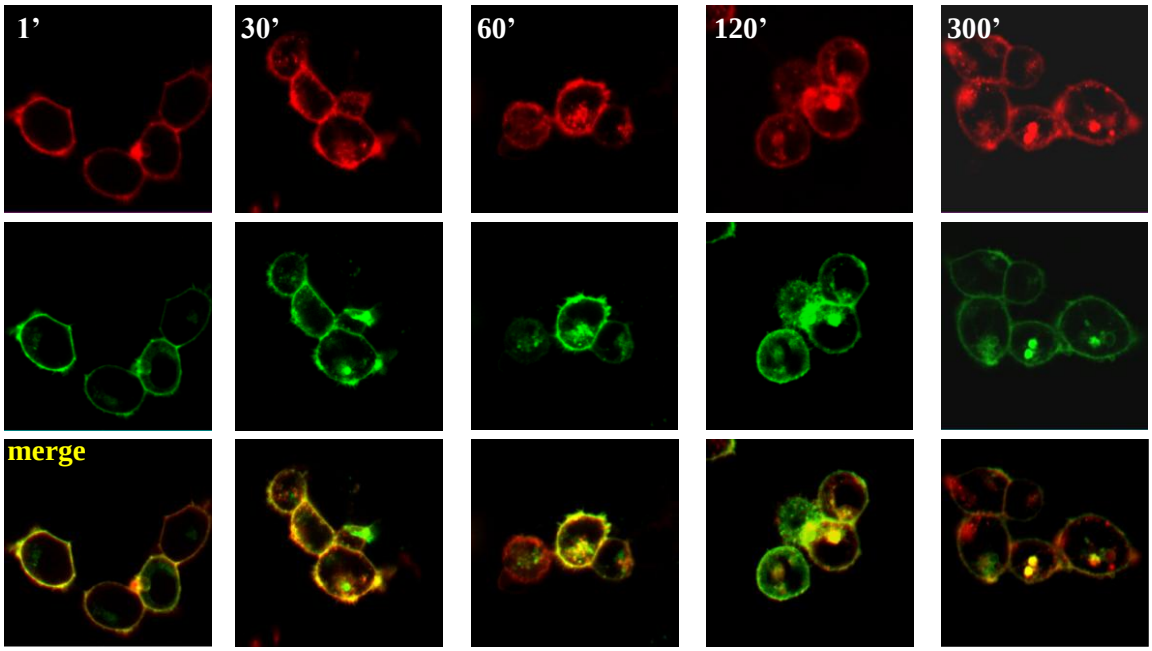

C:

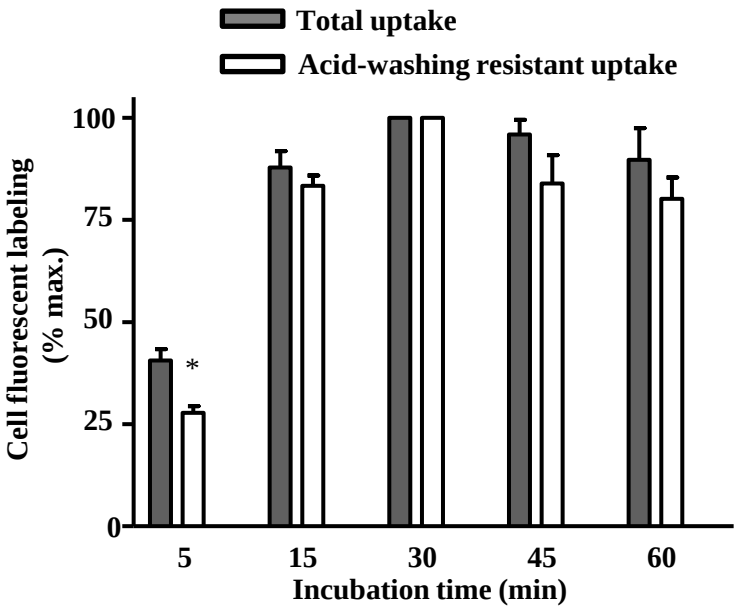

Fig. 1

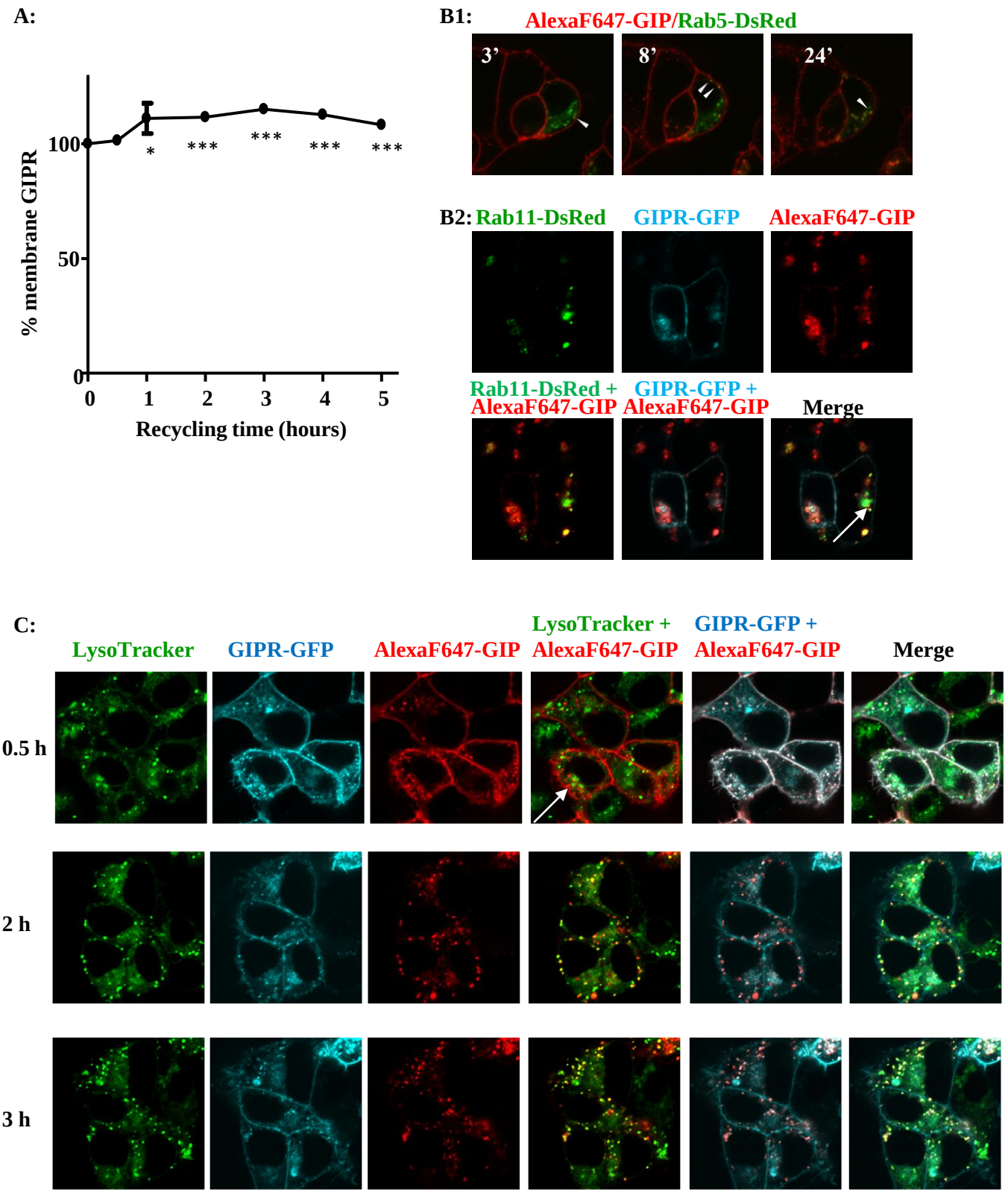
A:
% membrane GIPR
100
50
0
0
1
2
3
4
5
Recycling time (hours)
*
***
***
***
***
B1:
AlexaF647-GIP/Rab5-DsRed
3'
8'
24'
B2:
Rab11-DsRed
GIPR-GFP
AlexaF647-GIP
Rab11-DsRed +
AlexaF647-GIP
GIPR-GFP +
AlexaF647-GIP
Merge
C:
LysoTracker
GIPR-GFP
AlexaF647-GIP
LysoTracker +
AlexaF647-GIP
GIPR-GFP +
AlexaF647-GIP
Merge
0.5 h
2 h
3 h

Fig. 2

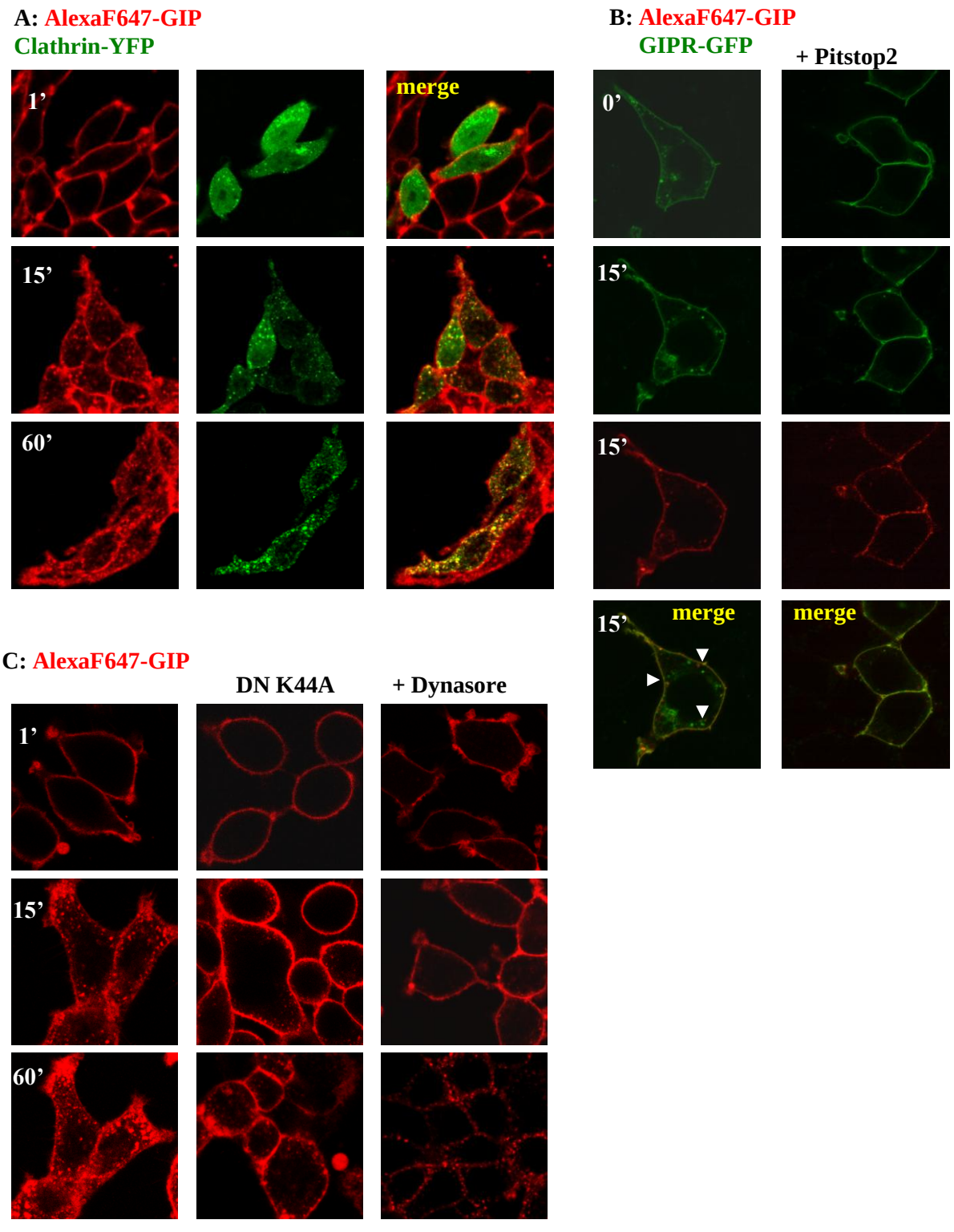
A: AlexaF647-GIP
Clathrin-YFP
1'
merge
15'
60'
B: AlexaF647-GIP
GIPR-GFP
+ Pitstop2
0'
15'
15'
15'
merge
merge
C: AlexaF647-GIP
DN K44A
+ Dynasore
1'
15'
60'

Fig. 3

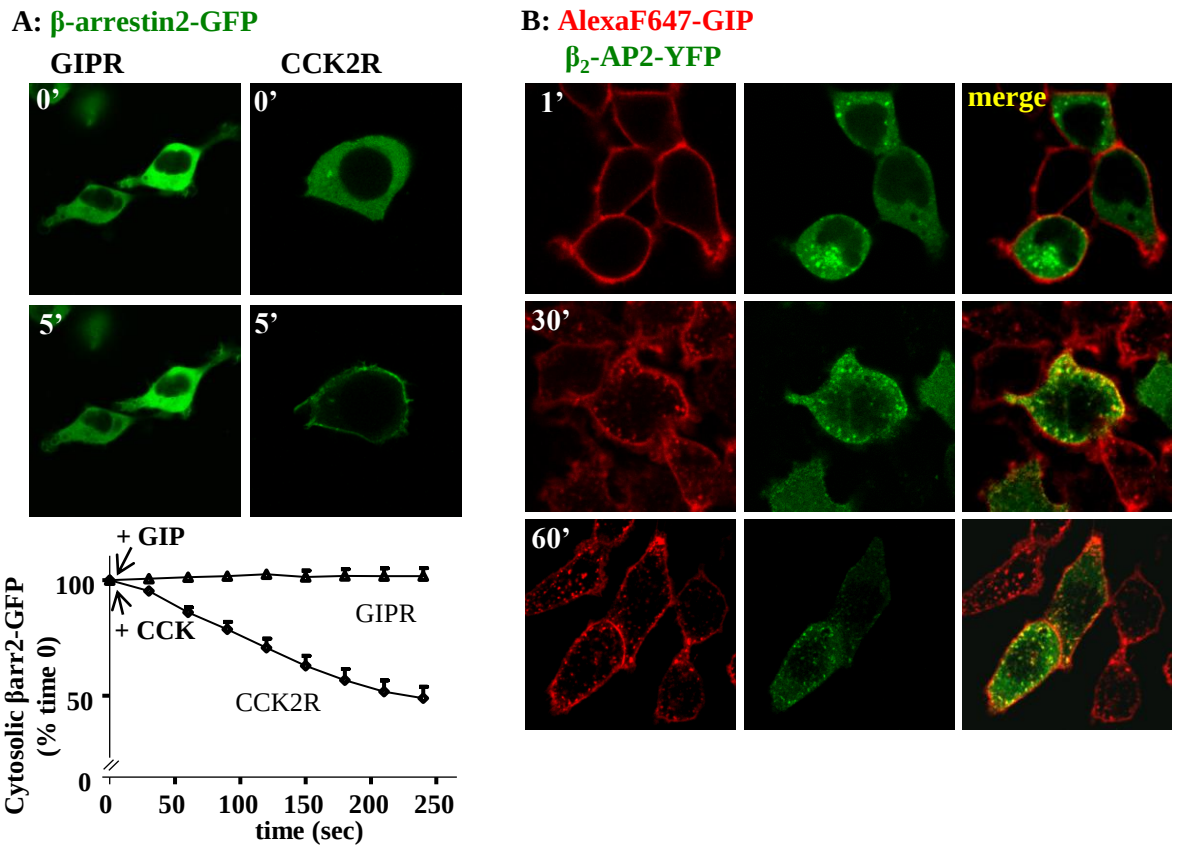
A: β-arrestin2-GFP
GIPR
CCK2R
0'
0'
5'
5'
+ GIP
+ CCK
GIPR
CCK2R
Cytosolic βarr2-GFP
(% time 0)
100
50
0
0
50
100
150
200
250
time (sec)
B: AlexaF647-GIP
β2-AP2-YFP
1'
merge
30'
60'

Fig. 4

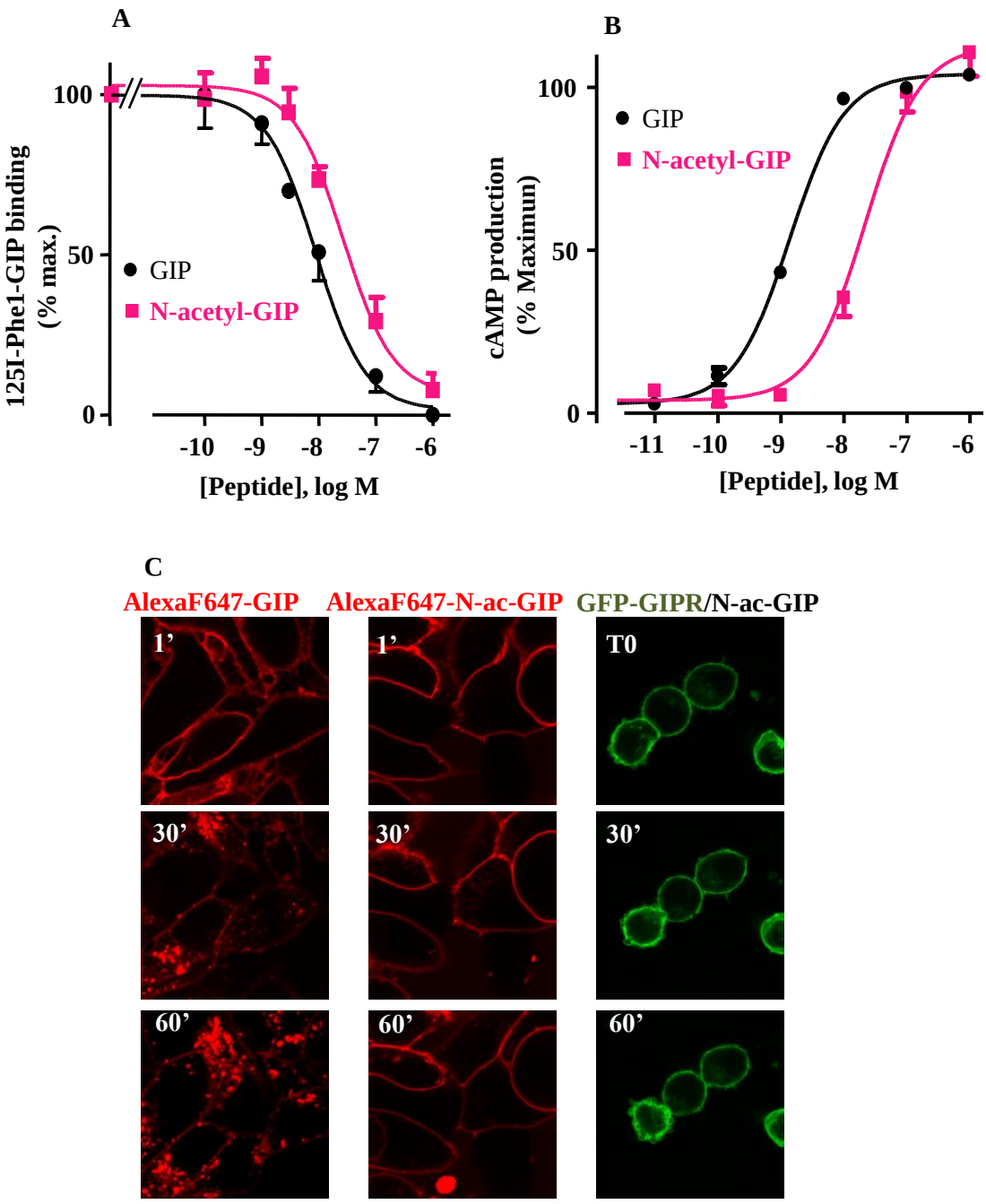
A
125I-Phe1-GIP binding
(% max.)
100
50
0
GIP
N-acetyl-GIP
-10
-9
-8
-7
-6
[Peptide], log M
B
cAMP production
(% Maximun)
100
50
0
GIP
N-acetyl-GIP
-11
-10
-9
-8
-7
-6
[Peptide], log M
C
AlexaF647-GIP
AlexaF647-N-ac-GIP
GFP-GIPR/N-ac-GIP
1'
1'
T0
30'
30'
30'
60'
60'
60'

Fig. 5

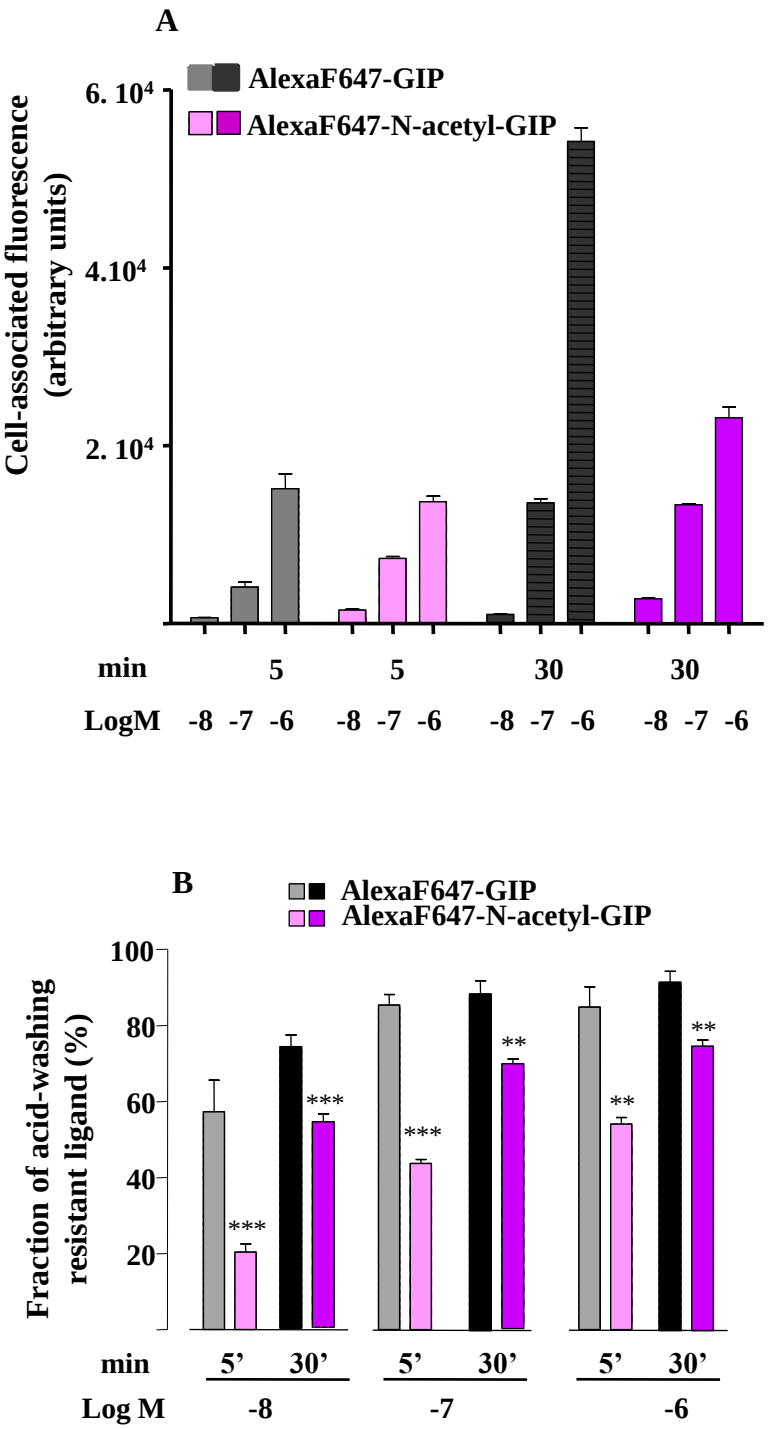
A
AlexaF647-GIP
AlexaF647-N-acetyl-GIP
Cell-associated fluorescence (arbitrary units)
6. 10⁴
4.10⁴
2. 10⁴
min
5
5
30
30
LogM
-8 -7 -6 -8 -7 -6 -8 -7 -6 -8 -7 -6
B
AlexaF647-GIP
AlexaF647-N-acetyl-GIP
Fraction of acid-washing resistant ligand (%)
100
80
60
40
20
***
***
***
**
**
**
min
5' 30' 5' 30' 5' 30'
Log M
-8
-7
-6

Fig. 6

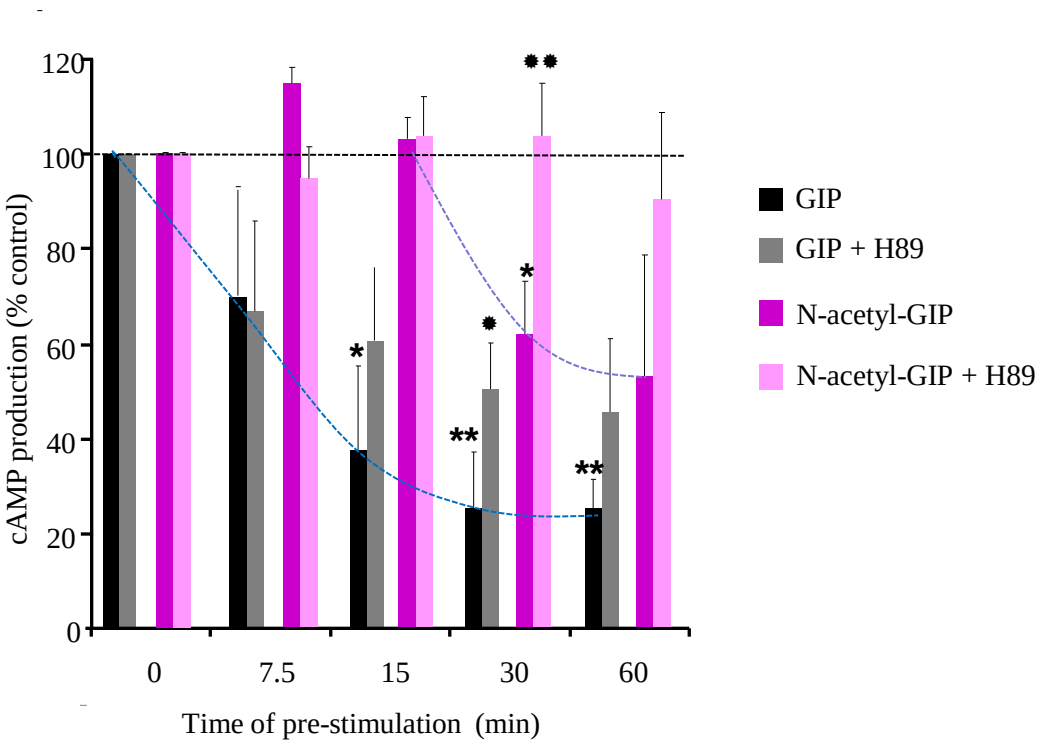
120
100
80
60
40
20
0
cAMP production (% control)
0
7.5
15
30
60
Time of pre-stimulation (min)
GIP
GIP + H89
N-acetyl-GIP
N-acetyl-GIP + H89

Fig. 7

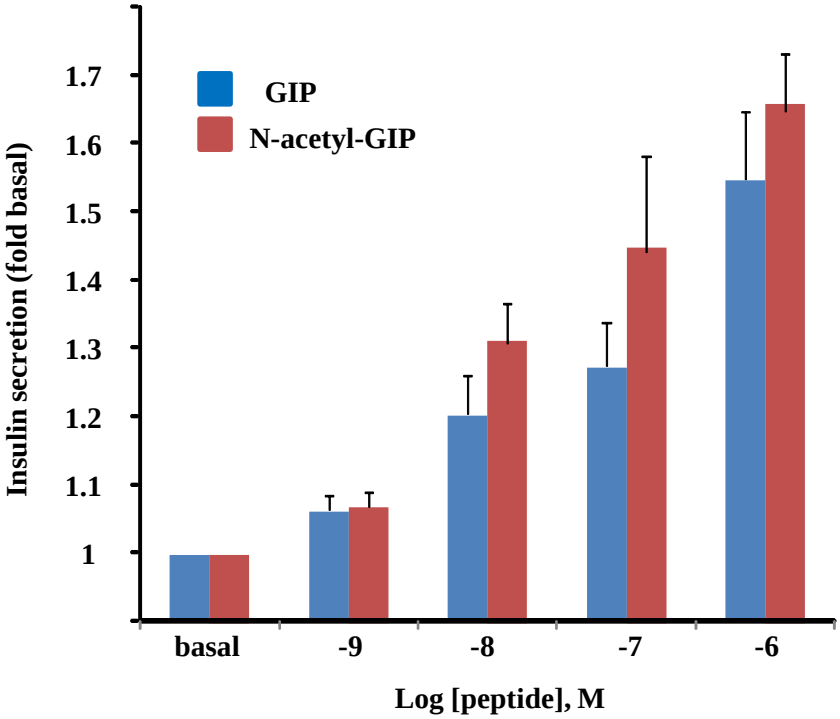
GIP
N-acetyl-GIP
Insulin secretion (fold basal)
1.7
1.6
1.5
1.4
1.3
1.2
1.1
1
basal
-9
-8
-7
-6
Log [peptide], M

Fig. 8

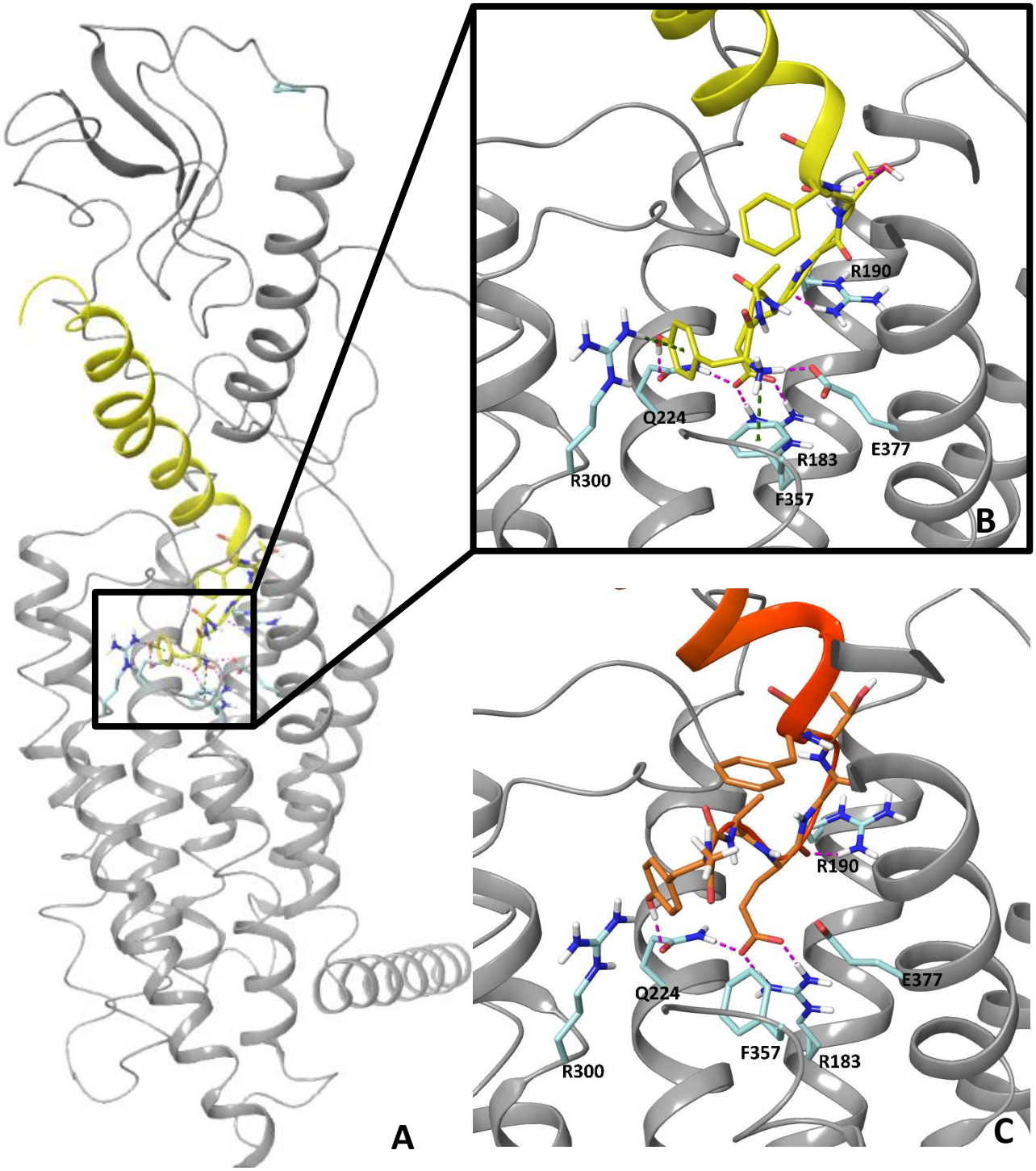
R190
Q224
R183
E377
R300
F357
B
A
R190
E377
Q224
F357
R183
R300
C

Fig. 9

Highlights

Glucose-Insulinotropic Polypeptide receptor (GIPR) is an incretin receptor subjected to strong regulation.>GIPR internalization is robust and rapid, it involved clathrin-coated pits, AP-2 and dynamin.>Neither GIPR C-terminal region nor β-arrestin1/2 are required for GIPR internalization.>N-acetyl-GIP weakly stimulates GIPR internalization and desensitization of cAMP response.>N-acetyl-GIP interacts more slightly than GIP with residues of helices 6 and 7 of GIPR.

Supplementary Data to article:Internalization and desensitization of the human glucose-dependent-insulinotropic receptor is affected by N-terminal acetylation of the agonist by Sadek Ismail et al.

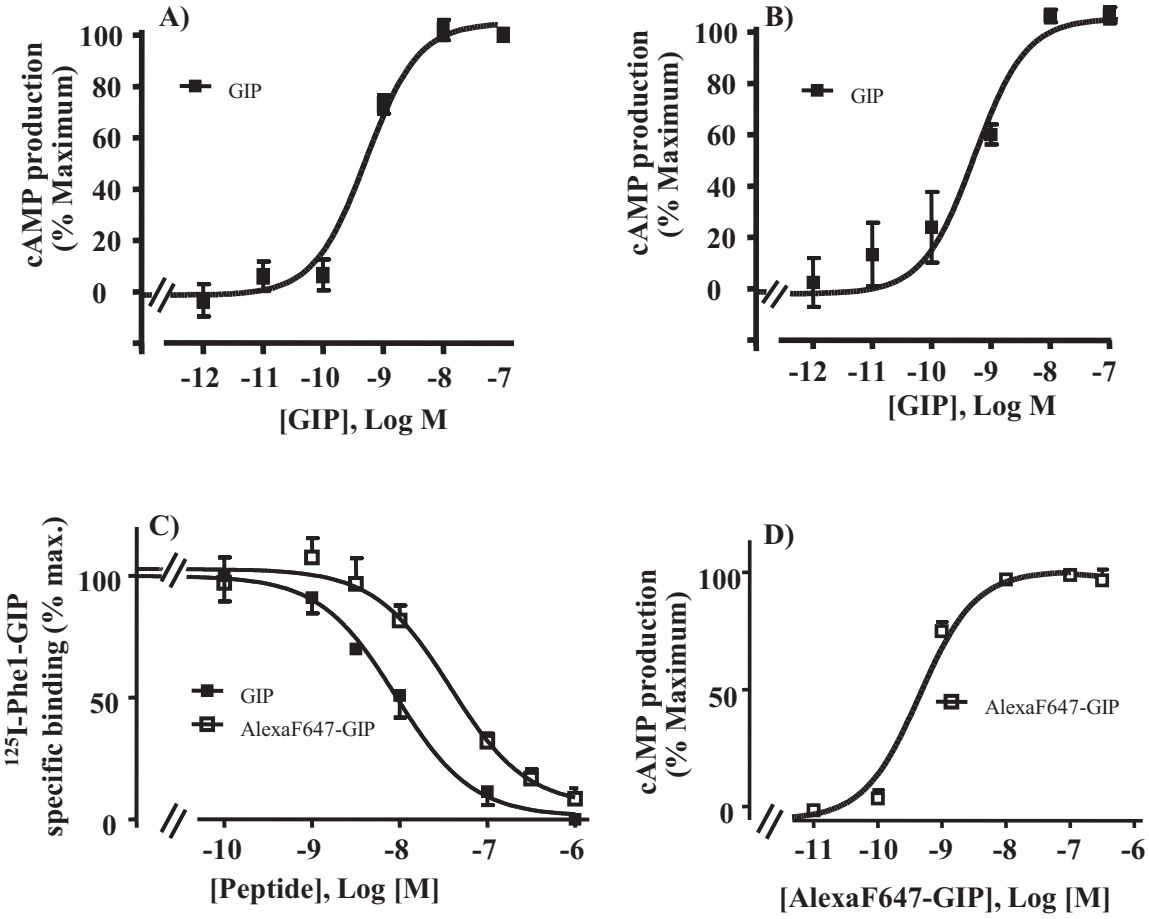

Fig. 1S: Functional and binding characterization of cells expressing GIP receptors and fluorescent labeled GIP. **Panel A,** Flp-In™ HEK-GIPR stably expressing human GIPR were transfected with EPAC Bret sensor or in **panel B**, HEK293T cells co-expressing transiently GIPR and EPAC Bret sensor were stimulated with GIP at indicated concentrations for 5 min. cAMP production was assayed by BRET as described in materials and methods. Concentration of GIP giving half-maximal stimulation of cAMP production were 0.53 ± 0.17 nM in Flp-In™ HEK-GIPR cells and 0.52 ± 0.06 nM in HEK293T-GIPR cells. **Panel C**, Flp-In™ HEK-GIPR were incubated with ^{125}-I-Phe1-GIP in the presence of increasing concentrations of GIP or AlexaF647-GIP for 30 min. Results are mean ± SEM of 4 individual experiments. Analysis of inhibition curves provides the following Ki: 11.3 ± 3.1 nM for GIP and 25.5 ± 5.7 nM for AlexaF647-GIP. **Panel D**, HEK293T cells co-expressing transiently GIPR and EPAC Bret sensor were stimulated with AlexaF647-GIP at indicated concentrations for 5 min and cAMP production was assayed by BRET. Results are mean ± SEM of 3 individual experiments. AlexaF647-GIP stimulated cAMP production with an EC_{50} of 0.47 ± 0.08 nM.

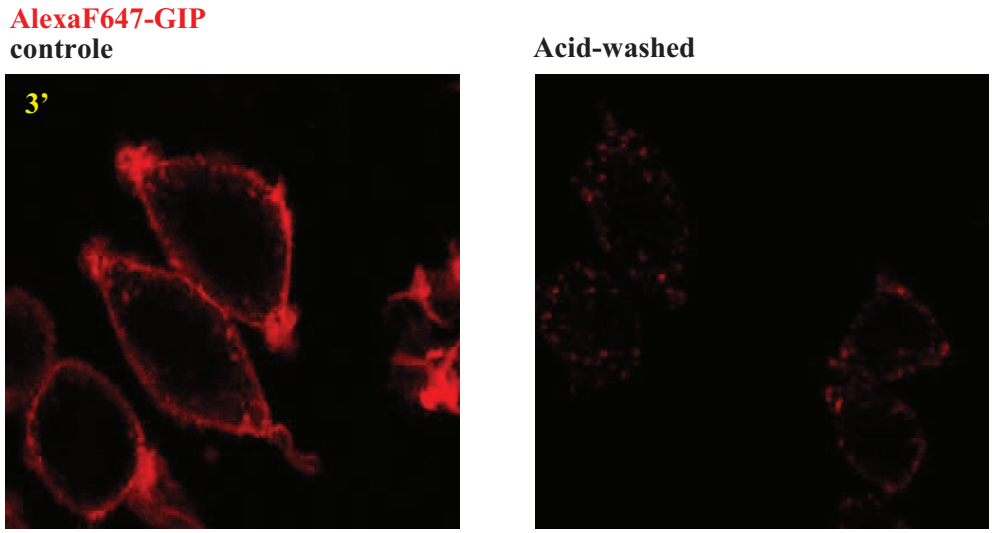

Fig. 2S: Acid-washing of membrane-bound but not internalized AlexaF647-GIP.
Flp-In™ HEK-GIPR were incubated with AlexaF647-GIP (100 nM) for 2-3 min. at 37°C. Then, cells were acid-washed (B) or not at 4°C for 5 min. Confocal microscopy images show efficiency of the elimination of membrane-bound fluorescent GIP and some remaining sequestered or internalized ligand.

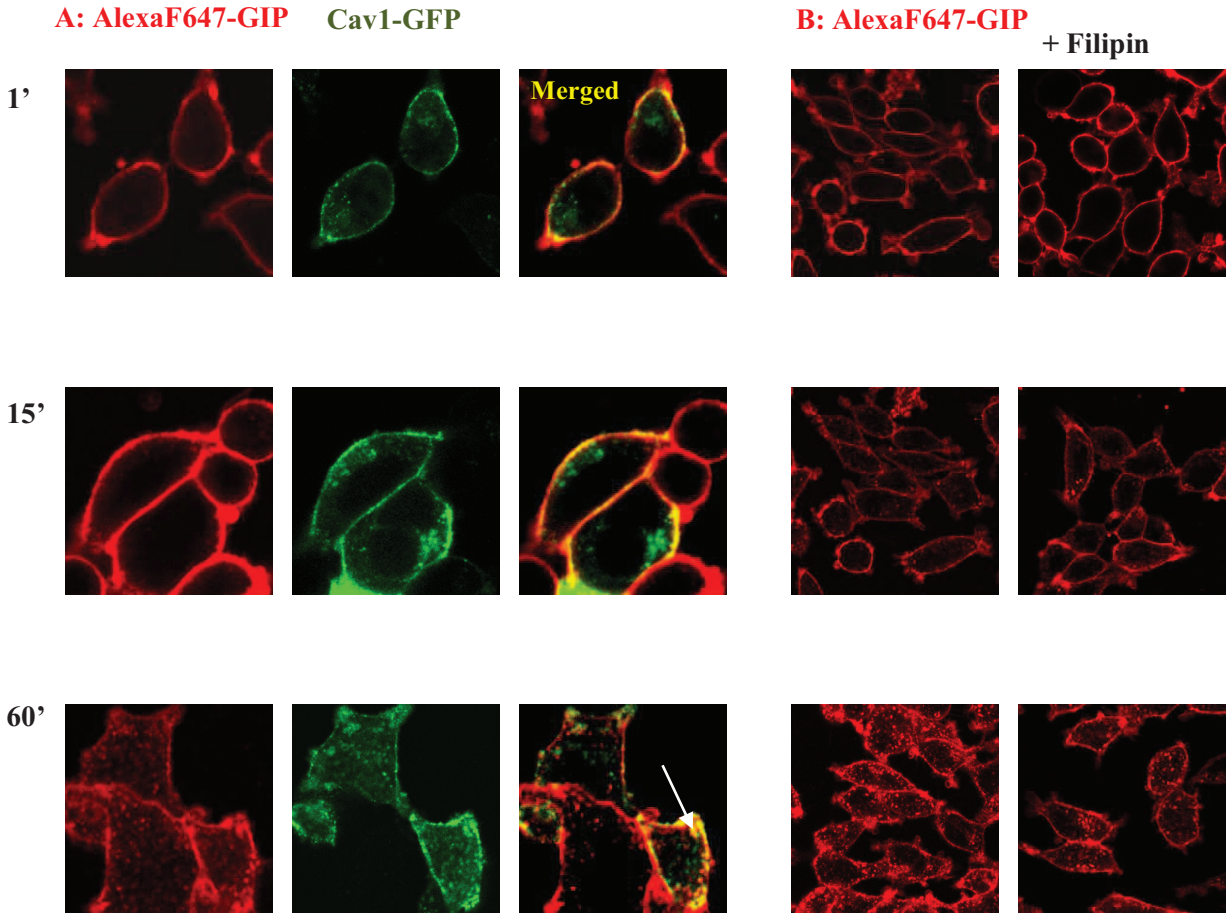

Fig. 3S: GIP receptor does not significantly internalize through caveolae.
Right panels: Flp-InTM HEK-GIPR cells were incubated with AlexaF647-GIP alone or in the presence of the caveola inhibitor, fillipin (50µM). **Left panels**: HEK 293T cells co-transfected with cDNA encoding GIPR and caveoline1-GFP were stimulated with AlexaF647-GIP for indicated times. Images show no significant change of internalization of GIPR in the presence of fillipin. AlexaF647-labeled GIPR strongly co-localizes with caveoline1-GFP at the plasma membrane and in some cases in endocytosic vesicles (the white arrow shows an example).

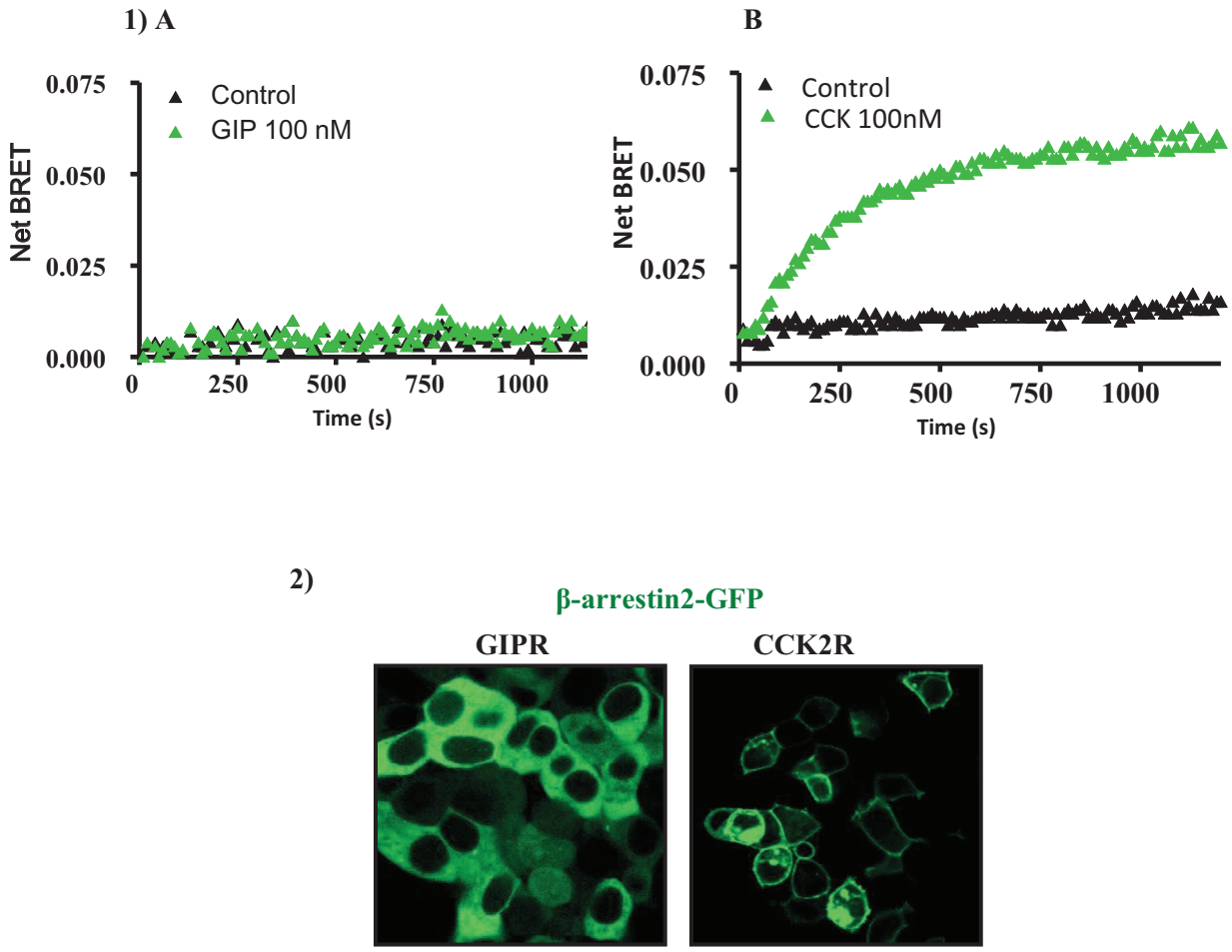

Fig. 4S: Absence of β-arrestin1/2 recruitment to GIP receptor

1) BRET assays showing absence of direct recruitment of β-arrestin2 to GIP receptor.

Panel A: HEK293 T cells co-transfected with GIPR-RLuc and β-arrestin2-YFP were stimulated with GIP (100 nM). Panel B: HEK293 T cells co-transfected by CCK2R-RLuc and β-arrestin2-YFP were stimulated with CCK (100 nM). Results are those from one representative experiment of 3 others and are expressed as netBRET.

2) Confocal microscopy images of Flp-In™ HEK-GIPR cells or Flp-In™ HEK-CCK2R transfected with β-arrestin2-GFP stimulated with GIP or CCK (100 nM), respectively. Images show that β-arrestin2-GFP remains in the cytoplasm in stimulated Flp-In™ HEK-GIPR cells whereas it was translocated to the plasma membrane in stimulated Flp-InTM HEK-CCK2R cells used as positive control of β-arrestin2 recruitment.

A: cAMP production

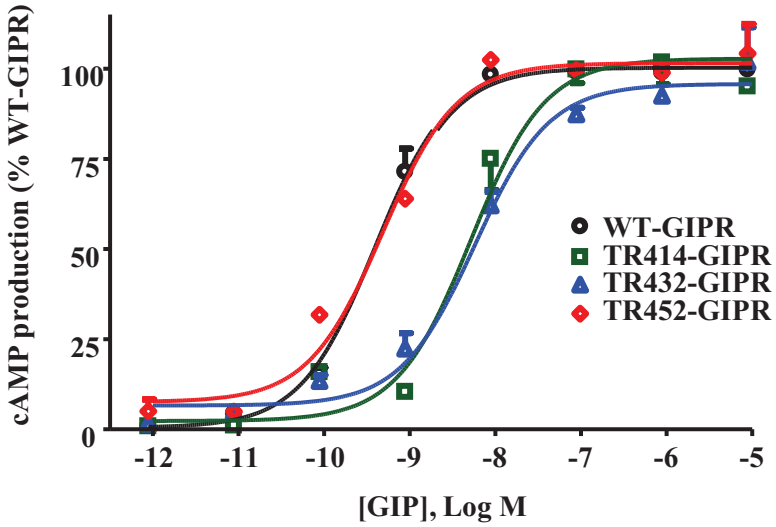

B: AlexaF647-GIP

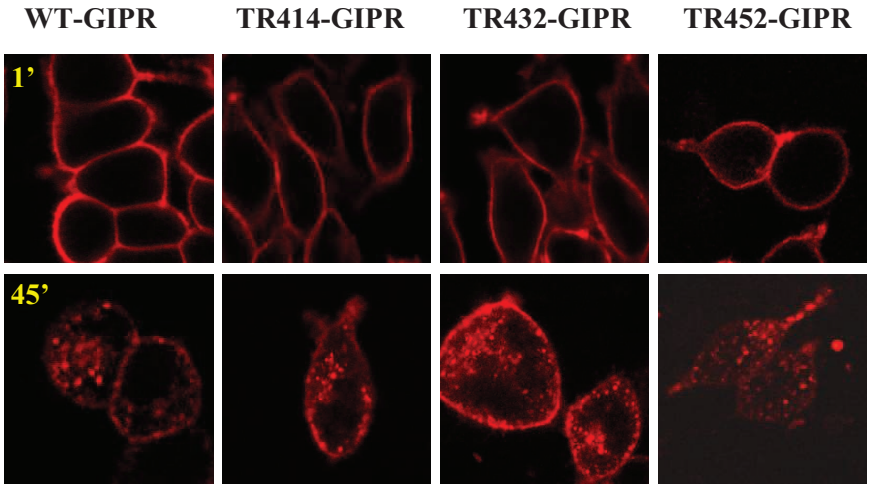

C: Quantification of internalized AlexaF647-GIP

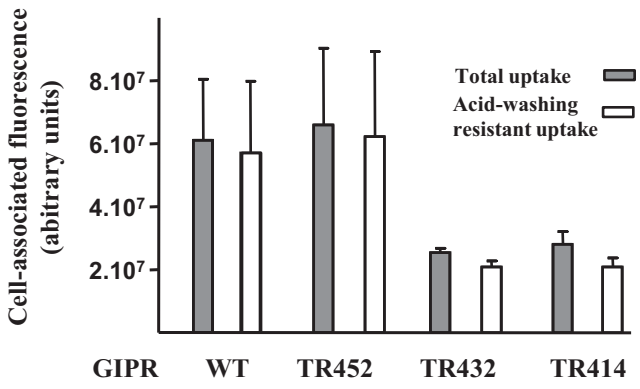

Fig. 5S: The C-terminal region of the GIP receptor is dispensable for internalization of GIP receptor.
A: C-terminal truncated GIP receptors retain ability to stimulate adenylyl cyclase.
HEK293 T cells co-transfected with EPAC BRET biosensor and with wild-type or truncated GIPR positions 414, 432 or 452 (termed TR414, TR432, TR452) were stimulated with increasing concentrations of GIP. BRET was measured 5 min. after addition of GIP. Almost identical maximal responses were observed with wild-type and truncated GIPR. Potencies to stimulate production of cAMP were as follow: $EC_{50,}$ Wild-type GIPR: 0.27 ± 0.21, TR414: 5.2 ± 0.1 nM, TR432: 5.8 ± 0.1 nM, TR452: 0.48 ± 0.25 nM.
B: C-terminal truncated GIP receptors abundantly internalize upon stimulation with AlexaF647-GIP.
HEK293 T cells transfected with wild-type GIPR or with TR414-, TR432-, TR452-GIPR were stimulated with AlexaF647-GIP (100 nM). Confocal microscopy images show that all truncated GIPR abundantly internalized upon GIP stimulation (shown at 45 min).
C: Quantification of AlexaF647-GIP internalization indicates that the C-terminal region of the GIP receptor is dispensable for internalization of GIP receptor. Two batches of HEK293 T cells transfected with wild-type GIPR or with TR414-, TR432-, TR452-GIPR were stimulated with AlexaF647-GIP (100 nM) for 30 min. Uptake of ligand was stopped by cooling the cells on ice. After PBS washing at 4°C, one batch was acid-washed whereas the second batch was PBS-washed (4°C). Fluorescence remaining associated to cells was quantified by FACS.

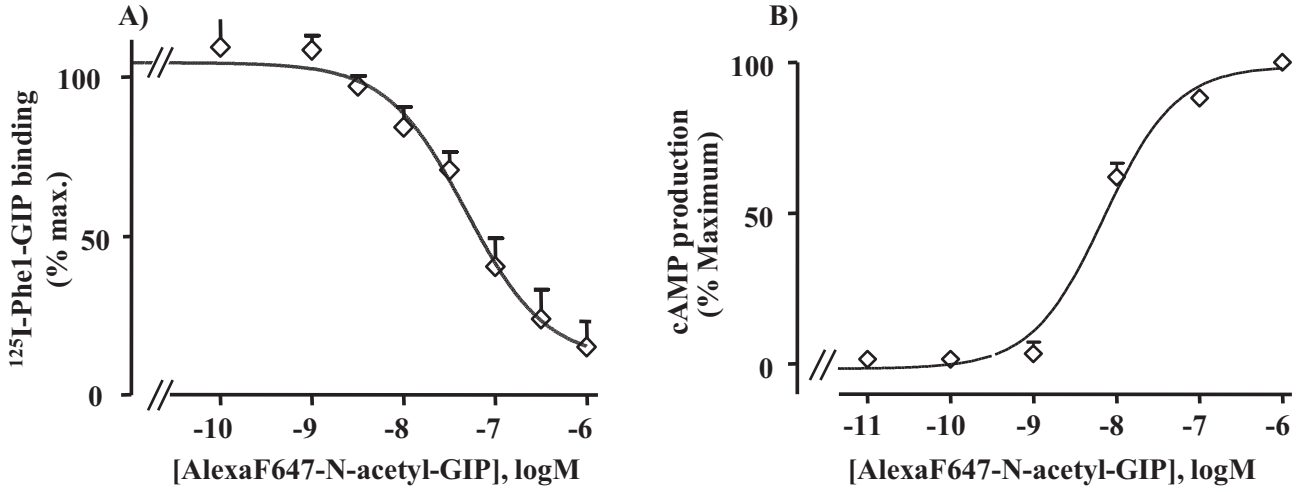

Fig. 6S: Pharmacological properties of N-acetyl-GIP and AlexaF647-N-acetyl-GIP
Panel A: **Competition binding between ^{125}I-Phe1-GIP and AlexaF647-N-acetyl-GIP.** Flp-In^{TM} HEK-GIPR were incubated with ^{125}-I-Phe1-GIP (100 pM) in the presence of increasing concentrations of AlexaF647-N-acetyl-GIP for 30min. Results are mean ± SEM of 4 individual experiments. Inhibition constant of AlexaF647-N-acetyl-GIP was: 49.5 ± 5.8 nM. **Panel B: Dose-response curve for stimulation of cAMP production by AlexaF647-N-acetyl-GIP.** HEK293T cells co-expressing transiently GIPR and EPAC Bret sensor were stimulated with AlexaF647-N-acetyl-GIP at indicated concentrations, for 5 min, and cAMP production was assayed by BRET. Results are mean ± SEM of 3 individual experiments and show that AlexaF647-N-acetyl-GIP stimulated cAMP production with an EC_{50} of 7.3 ± 0.9 nM.

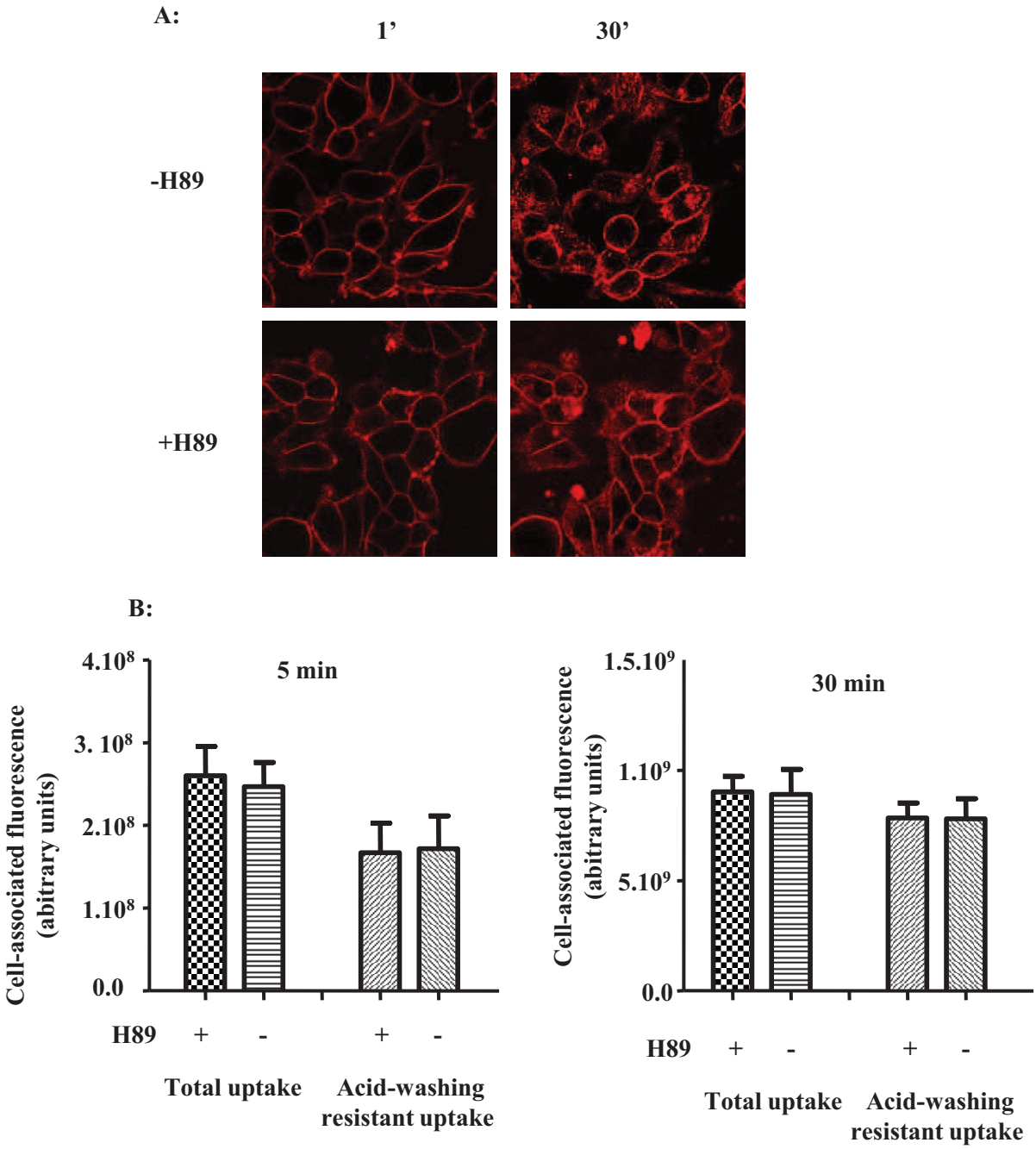

Fig. 7S: Absence of effect of H89, a PKA inhibitor, on GIP-stimulated internalization of the GIP receptor.
A: Flp-In™ HEK-GIPR cells were stimulated with AlexaF647-GIP (100 nM) in the absence or in the presence of H89. Confocal microscopy images show internalization of AlexaF647-GIP at 30 min).
B: The absence of effect of H89 on GIP-induced GIPR internalization was confirmed by acid-washing experiment which indicated that the same amount of AlexaF647-GIP was resistant to acid washing when internalization proceeded in the absence or in the presence of H89.